

SIMPLE CONFORMAL LOOP ENSEMBLES ON LIOUVILLE QUANTUM GRAVITY

JASON MILLER, SCOTT SHEFFIELD, AND WENDELIN WERNER

ABSTRACT. We show that when one draws a simple conformal loop ensemble (CLE_κ for $\kappa \in (8/3, 4)$) on an independent $\sqrt{\kappa}$ -Liouville quantum gravity (LQG) surface and explores the CLE in a natural Markovian way, the quantum surfaces (e.g., corresponding to the interior of the CLE loops) that are cut out form a Poisson point process of quantum disks. This construction allows us to make direct links between CLE on LQG, asymmetric $(4/\kappa)$ -stable processes, and labeled branching trees. The ratio between positive and negative jump intensities of these processes turns out to be $-\cos(4\pi/\kappa)$, which can be interpreted as a “density” of CLE loops in the CLE on LQG setting. Positive jumps correspond to the discovery of a CLE loop (where the LQG length of the loop is given by the jump size) and negative jumps correspond to the moments where the discovery process splits the remaining to be discovered domain into two pieces.

Some consequences of this result are the following: (i) It provides a construction of a CLE on LQG as a patchwork/welding of quantum disks. (ii) It allows to construct the “natural quantum measure” that lives in a CLE carpet. (iii) It enables us to derive some new properties and formulas for SLE processes and CLE themselves (without LQG) such as the exact distribution of the trunk of the general asymmetric $SLE_\kappa(\kappa - 6)$ processes.

The present work deals directly with structures in the continuum and makes no reference to discrete models, but our calculations match those for scaling limits of $O(N)$ models on planar maps with large faces and CLE on LQG. Indeed, our Lévy-tree descriptions are exactly the ones that appear in the study of the large-scale limit of peeling of discrete decorated planar maps such as in recent work of Bertoin, Budd, Curien and Kortchemski.

The case of non-simple CLEs on LQG will be the topic of another paper.

CONTENTS

1. Introduction	1
2. Background	11
3. Exploring CLEs on quantum half-planes	17
4. CLE explorations of quantum disks	23
5. The natural quantum measure in the CLE carpet	27
Appendix A. Proof of Lemma 3.3	34
References	36

1. INTRODUCTION

1.1. Background. The present work presents some new direct connections between conformal loop ensembles (CLE) and Liouville quantum gravity (LQG). Before describing our main results, let us give quick one-page surveys about each of the three main objects involved: CLE and their explorations; LQG surfaces; asymmetric stable processes and labeled trees.

Date: November 7, 2021.

1.1.1. *Background on CLE and on CLE explorations.* The *Schramm-Loewner evolutions* (SLE_κ) were introduced by Schramm in [44] and are individual random curves joining two boundary points of a simply connected domain. They are defined as an infinitely divisible iteration of independent random conformal maps and they are classified by a positive parameter κ . The SLE_κ curves turn out to be simple when $\kappa \leq 4$, and they have double points as soon as $\kappa > 4$ [43]. The *conformal loop ensembles* CLE_κ [46, 49] are random families of non-crossing loops in a simply connected domain D . In a CLE_κ , the loops are SLE_κ -type curves (for the same value of κ). While SLE_κ corresponds to the conjectural scaling limit of a single interface in a statistical physics model in a domain with some special boundary conditions involving two marked boundary points, CLE_κ is the conjectural scaling limit of the whole collection of interfaces with some uniform boundary conditions. It turns out that the CLE_κ can be defined only in the regime where $\kappa \in (8/3, 8)$. The phase transition at $\kappa = 4$ for SLE_κ curves is mirrored by the properties of the corresponding CLE_κ : When $\kappa \in (8/3, 4]$, which is the case that we will focus on in the present paper, the CLE_κ loops are all disjoint and simple. They conjecturally correspond to the scaling limit of dilute $O(N)$ models for $N \in (0, 2]$ (this is actually proved in the special case $N = 1$ which is the critical Ising model [50, 29, 20, 2]). The set of points that are surrounded by no CLE_κ loop is called the CLE_κ carpet. As shown in [49], these simple CLEs can be constructed in different ways, including via the so-called Brownian loop-soups. However, in the present work, we will use mostly the original SLE branching tree construction proposed in [46], and further studied and described in [49, 51, 39].

Let us give a brief intuitive description of some relevant results about the loop-trunk decomposition of (the totally asymmetric) branches of the SLE_κ branching tree (mostly from [39]) that will play an important role in the present paper: Suppose that $\kappa \in (8/3, 4)$, that one is given a CLE_κ in a domain D , and that one chooses two boundary points x and y . Then, it is possible to make sense of a random non-self-crossing curve (but with double points) from x to y , that (i) stays in the CLE carpet, (ii) always leaves a CLE loop to its right if it hits it, (iii) possesses some conformal invariance and locality properties. These three properties in fact characterize the law of the curve, so that it can be interpreted as the critical percolation interface from x to y in the CLE_κ carpet (loosely speaking, it traces the outer boundary of percolation clusters in this carpet that touch the clockwise part of the boundary from x to y). This process is called the CPI (conformal percolation interface) in the CLE_κ carpet.

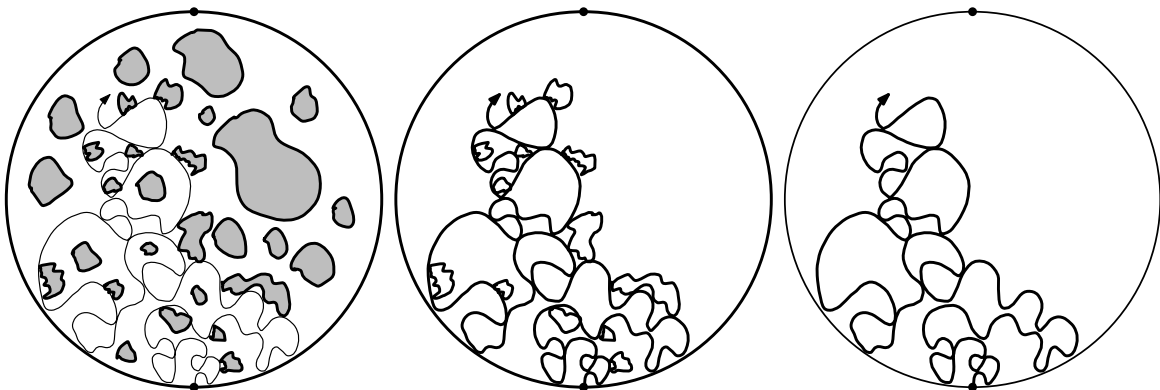


FIGURE 1. CPI in a CLE, the curve η and its trunk

The “quenched” law (i.e., averaged over all possible CLE_κ) of the CPI turns out to be the natural target-invariant version of $SLE_{\kappa'}$ for $\kappa' = 16/\kappa$, called a $SLE_{\kappa'}(\kappa' - 6)$ process. In the same way as

for ordinary percolation, it is actually possible to make sense of the whole branching tree of CPIs targeting from all the points in the domain.

As one can expect from the properties of CLEs, the law of the ordered family of CLE loops that a CPI branch encounters can be viewed as coming from a Poisson point process of SLE_κ type bubbles. The process that one obtains by tracing the CPI and the CLE loops along the way in the order in which they are encountered (this process is called the $\text{SLE}_\kappa(\kappa - 6)$ process), can be reconstructed from the collection of SLE_κ bubbles. The CPI is then called the *trunk* of this $\text{SLE}_\kappa(\kappa - 6)$ – see Figure 1. In [39], it is explained how to construct also this process by first sampling the entire CPI (which is an $\text{SLE}_{\kappa'}(\kappa' - 6)$ as mentioned above), and then only to attach the collection of discovered CLE loops to it – this is referred to as the *loop-trunk* decomposition of the (totally asymmetric) $\text{SLE}_\kappa(\kappa - 6)$.

1.1.2. *Quantum surfaces and quantum disks.* Before discussing some basics about LQG surfaces, let us emphasize one important point: There are two essentially equivalent approaches to LQG surfaces – one where one views it as a random metric and one where one views it in terms of a random area measure (or random lengths of some particular random curves). In the present paper, we will always stick to the latter one and will not need to know about the former (note that showing that the random area measure defines also a random distance is a non-trivial recent result (see [17] and [25, 22, 24, 23])).

Suppose that one is given a simply connected domain D in the complex plane (with $D \neq \mathbf{C}$) and an instance of the Gaussian free field (GFF) with Dirichlet boundary conditions on D , to which one adds some (possibly random and unbounded) harmonic function h_0 , and let h denote the obtained field (this includes for instance the case where h is a GFF with “free boundary conditions”). It is by now a classical fact that can be traced back at least to work by Høegh-Krohn [26] and Kahane [28] that when $\gamma \in (0, 2)$, it is possible to define an *LQG area measure* $\mu_h = \mu_{h,\gamma}$ that can loosely be viewed as having a density $\exp(\gamma h)$ with respect to Lebesgue measure (one precise definition goes via an approximation/renormalization procedure, see [19]). An important feature to emphasize is that the obtained area measure is conformally covariant, in the sense that the image of $\mu_{h,\gamma}$ under a conformal map Φ from D onto \tilde{D} will be the measure $\mu_{\tilde{h},\gamma}$, where \tilde{h} is the sum of a Dirichlet GFF in \tilde{D} with the harmonic function $\tilde{h}_0 = h_0 \circ \Phi^{-1} + Q \log |(\Phi^{-1})'|$, with $Q = (2/\gamma + \gamma/2)$. This conformal covariance was chosen to hold a.s. for a *fixed* conformal map in [19] and to hold a.s. simultaneously for *all* conformal maps in [48].

In the case that h_0 is chosen so that the obtained field h is absolutely continuous with respect to a realization of the GFF with free boundary conditions, a similar procedure can be used to define a measure on the boundary of D , that is referred to as the *LQG length measure* $\nu_h = \nu_{h,\gamma}$. This boundary length measure ν_h is in fact a deterministic function of the area measure μ_h (it is in some sense its “trace on the boundary” and it is a deterministic function of the random function h_0). Again, this boundary LQG length measure turns out to be conformally covariant in the same way the LQG area measure is. This leads to the definition of a *quantum surface*, which is an equivalence class of distributions where distributions h, \tilde{h} are equivalent if there exists a conformal transformation Φ so that $h = \tilde{h} \circ \Phi^{-1} + Q \log |(\Phi^{-1})'|$. When one speaks of a quantum surface, it therefore means a distribution modulo this change of coordinate rule. A representative from the equivalence class is an *embedding* of a quantum surface.

Another important feature, pioneered in [47, 18] and extensively used in all the subsequent LQG/SLE papers is that when $\kappa = \gamma^2$ and $\kappa' = 16/\kappa$ (we will keep these relations throughout the paper),

then when one draws SLE_κ -type curves in D or $\text{SLE}_{\kappa'}$ -type curves in D that are independent of the field h , then it is possible to make sense (again in a conformally invariant way) of their LQG length – which therefore provides a way to parameterize the curve using the additional random input provided by h .

It turns out that some special choices for the random harmonic function h_0 are particularly interesting. One of these choices gives rise to the so-called γ -quantum disks. One property of quantum disks (for $\gamma \in (0, 2)$) is that almost surely, the total area measure is finite and the total boundary length is finite. It is actually convenient to work with either the probability measure P_L on quantum disks with a given boundary length L , or with the infinite measure on quantum disks $M = \int P_L dL/L^{\alpha+1}$, where here and in the sequel, α and γ are related by $\alpha = 4/\gamma^2 = 4/\kappa$. The measure P_L can be obtained from P_1 by adding $\frac{2}{\gamma} \log L$ to the field, which has the effect of multiplying the boundary length measure by the factor L and the area measure by the factor L^2 .

1.1.3. *Relevant Lévy processes and fragmentation processes.* Recall that when $\alpha \in (0, 2) \setminus \{1\}$, it is possible to define a real-valued stable process X of index α with no negative jumps. For such a process X started from 0, the processes $(X_{ct})_{t \geq 0}$ and $(c^{1/\alpha} X_t)_{t \geq 0}$ have the same law for all $c > 0$. The ordered collection of jumps of X will form a Poisson point process with intensity $dh/h^{1+\alpha}$ on \mathbf{R}_+ (or more precisely with intensity $dt dh/h^{1+\alpha}$ on $(0, \infty) \times (0, \infty)$, and the obtained process will make a jump h_i at time t_i for each (t_i, h_i) in this point process). The sum of all the small jumps accomplished before time 1 say is infinite when $\alpha \in (1, 2)$ (which is in fact the case that will be relevant to the present paper), but the process is nevertheless well-defined as a deterministic function of the Poissonian collection of jumps via Lévy compensation (it is the limit as $\epsilon \rightarrow 0$ of the process obtained by summing all the jump of X of size at least ϵ with the deterministic function $-c_\epsilon t$ for a well-chosen c_ϵ that goes to ∞ as $\epsilon \rightarrow 0$).

By considering the linear combination $X := U'X' - U''X''$ of two independent such stable processes X' and X'' with no negative jumps for $U' \geq 0, U'' \geq 0$, one then gets a general stable process for which the ratio between the average number of its negative and positive jumps is $U := U'/U'' \in [0, \infty]$. In the case where $U = 1$, this is a symmetric stable process.

In the context of fragmentation-type processes, it appears natural to consider variants of these stable processes that are tailored so that they remain positive at all times. The idea is that if the process is at x , then the rates at which it jumps to $x+h$ and $x-h$ will not be proportional to $1/h^{1+\alpha}$ anymore, but will also depend on x . Let us illustrate this with the following example that will be relevant in the present paper. Consider $\alpha \in (1, 2)$ and an asymmetric stable Lévy process X started from $x_0 > 0$ with index α and asymmetry parameter U as defined above. Recall that when the process X is at x , the rate at which it jumps to $x+h$ and $x-h$ respectively does not depend on x and is $U'/h^{1+\alpha}$ and $U''/h^{1+\alpha}$. It is possible to define a variant Y of X started from some positive y_0 , such that when the process is at y , the rate of jumps to $y+l$ and to $y-l$ respectively with the rates

$$\frac{U'y^{\alpha+1}}{l^{\alpha+1}(y+l)^{\alpha+1}} \quad \text{and} \quad \frac{U''y^{\alpha+1}}{l^{\alpha+1}(y-l)^{\alpha+1}} \mathbf{1}_{l < y/2}.$$

Note that this tends to diminish the rate of the positive jumps and to favor the negative ones (of size smaller than $l/2$) when compared to X , but that for very small $|l|$, the rates of jumps of Y are close to those of X . It is then easy to check that for all positive r and T , if $E_{T,r}$ denotes the event that the process remains larger than r up to time T , then the law of $(Y_t, t \leq T)$ on the event $E_{T,r}$ will be absolutely continuous with respect to that of $(X_t, t < T)$ on $E_{T,r}$, and to determine its Radon-Nikodym derivative. This allows one to define the process Y up to its first hitting time of 0

(which can be infinite). This process can have positive jumps of any size, but it can never more than halve itself during a jump.

The previous condition $l < y/2$ in the negative jumps of Y comes from the fact that the process Y is in fact naturally related to a fragmentation process that can be understood as follows: The negative jumps $y \mapsto y - l$ correspond to the splitting of particle of mass y into two particles of masses l and $y - l$ respectively. Then, the two particles will evolve independently. In this setup, the process Y corresponds to the fact that at each such splitting within this random branching process \mathcal{T} , one follows only the evolution of the largest of the two offspring. But, by using a countable collection of independent copies of Y , it is then also possible to define the evolutions of all the other offspring and their offspring – and to define an entire fragmentation process \mathcal{T} . This is a random labeled tree-like structure, of a type that has been subject of extensive studies, see e.g., [4, 5] and the references therein, and that is also sometimes referred to as multiplicative cascades, and related to branching random walks as initiated by Biggins [8].

The positive jumps of Y can just be kept as they are (the particle of mass y becomes a particle of mass $y + l$) as in \mathcal{T} above, or alternatively also viewed as a splitting into the creation of two particles of masses $y + l$ and l respectively that then evolve independently (and this therefore gives rise to a larger tree structure $\tilde{\mathcal{T}}$).

It should be noted that this tree \mathcal{T} appears already in the asymptotic study of peeling processes on some planar maps, see [13, 5] and the references therein.

1.2. Results of the present paper.

1.2.1. *CLEs on quantum disks.* We now begin to describe the results of the present paper about explorations of a CLE_κ drawn on an independent quantum disk. Here and throughout this introduction, we suppose that $\kappa \in (8/3, 4)$ and we define (and we will use these relations throughout this introduction)

$$(1.1) \quad \gamma := \sqrt{\kappa}, \quad \kappa' := \frac{16}{\kappa}, \quad \text{and} \quad \alpha := \frac{4}{\kappa}.$$

Consider a γ -quantum disk of boundary length y_0 parameterized by a simply connected domain D – and let m be a boundary point, chosen uniformly according the LQG boundary length measure. Consider on the other hand an independent CLE_κ in D .

One can then define a CLE exploration tree starting from m (recall [40] that tracing such a tree involves yet additional randomness as it loosely speaking amounts to exploring CPI percolation paths within the CLE carpet) as described above – which gives rise to a CLE_κ exploration tree, or equivalently to the $\text{SLE}_\kappa(\kappa - 6)$ branching tree. One can recall that independent SLE_κ and $\text{SLE}_{\kappa'}$ -type curves drawn in a γ -quantum disk both have a natural LQG length [47, 18]. So in particular:

- Each CLE loop, which is an SLE_κ type loop will have its LQG length.
- Each CPI branch, which is an $\text{SLE}_{\kappa'}$ type curve can be parameterized by a constant multiple of its LQG-length, which is implicitly what we will do in the following paragraphs.
- The boundaries of the connected components of the complement of an $\text{SLE}_\kappa(\kappa - 6)$ curve at a given time, which are SLE_κ -type curves will also be equipped with their LQG length measure.

In particular, we see that:

- When the CPI hits a CLE loop for the first time, then if one attaches the whole CLE loop at once, one splits a domain with boundary length l into two domains with boundary length $l + y$ and y , where y denotes the quantum length of the CLE loop (the domain O_l with boundary length y would correspond to the inside of the discovered CLE loop), see Figure 2.

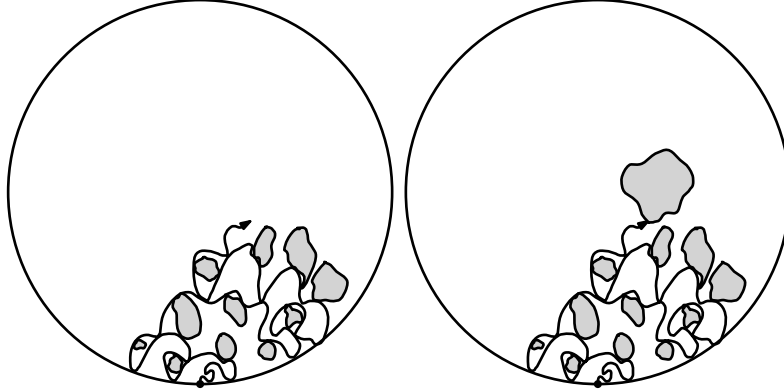


FIGURE 2. When the trunk of the CPI from $-i$ to i hits a CLE loop, the boundary length of the remaining to be explored domain makes a positive jump

- When the CPI (i.e., the $SLE_{\kappa'}(\kappa' - 6)$ process which is the trunk of the $SLE_{\kappa}(\kappa - 6)$) disconnects the remaining-to-be-explored domain into two pieces (this can happen for instance when it hits ∂D), then it splits the remaining-to-be explored domain of boundary length y into two domains of boundary lengths y_1 and y_2 where $y_1 + y_2 = y$ (i.e. into one domain with boundary length l and one with boundary length $y - l$, where $l < y/2$), see Figure 3.

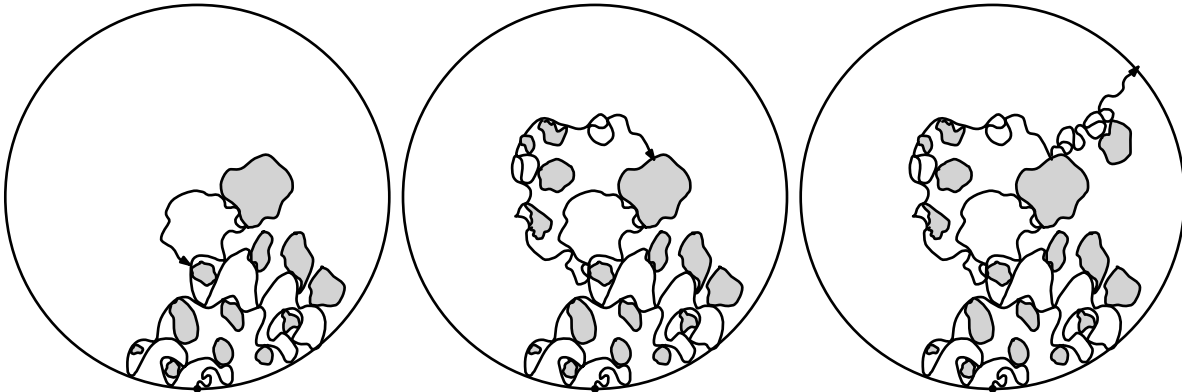


FIGURE 3. Examples of configurations when the exploration process splits the to-be-explored domain into two pieces

In this way, when one discovers this “CLE on LQG” structure via the CPI tree (and when one hits a CLE for the first time, one discovers it entirely), then one gets a fragmentation tree type-structure. It turns out to be handy to use the LQG length of the CPI branches as time-parameterizations for the tree structure. At any time along one branch, the label is the boundary length of the remaining to be discovered domain that this branch is currently discovering. If one follows one branch of the

tree, these labels will have positive jumps that correspond to the discovery of a CLE_κ loop, and negative jumps that correspond to times at which the CPI splits the remaining-to-be-discovered domain into two pieces.

Our first main statement goes as follows:

Theorem 1.1 (Exploration tree of a CLE on a quantum disk). *The law of the obtained fragmentation tree (obtained from drawing a CLE exploration on an independent LQG disk as just described) is exactly that of the fragmentation tree-structure \mathcal{T} described above, with*

$$U = -\cos(\pi\alpha) = -\cos(4\pi/\kappa).$$

Furthermore, conditionally on \mathcal{T} , the quantum surfaces encircled by the CLE_κ loops are independent quantum disks (the boundary length of which are given by the jumps in \mathcal{T}).

As a consequence, one for instance gets that the joint law of all the LQG lengths of all CLE_κ loops in a quantum disk is the same as the collection of all the positive jumps appearing in \mathcal{T} .

We now give an equivalent reformulation of this theorem in terms of the law of one branch of the exploration tree. Suppose that one traces the particular branch of the exploration tree (parameterized by its LQG length) using the following rule: Whenever the trunk disconnects the remaining-to-be-discovered domain into two pieces, one continues exploring the branch of the tree in the domain with largest boundary length. At such a time, the boundary-length L_t of the remaining to be discovered domain makes a negative jump from y to some $y - l$ with $l < y/2$ — and when the CPI discovers a CLE loop for the first time, this process has a positive jump of size given by the boundary length of that loop.

Theorem 1.2 (Branch of the exploration tree of CLE on a quantum disk). *The law of this process L is the law of the process Y described above, with the relation $U = -\cos(\pi\alpha)$. Furthermore, conditionally on the collection of jumps of L , the law of the quantum surfaces that are cut out by the trunk of the $\text{SLE}_\kappa(\kappa - 6)$ process (corresponding to the negative jumps of Y) and of the inside of the discovered CLE loops (that correspond to the positive jumps of Y) are all independent quantum disks.*

1.2.2. *The natural LQG area measure in the CLE carpet.* The previous description of the exploration mechanism in a quantum disk makes it possible to reduce many questions to computations for these labeled Lévy trees, for which there exists a rather substantial literature, including recent results motivated by the study of planar maps with large faces [30, 6, 5, 15].

We illustrate this here by constructing the natural LQG-measure that is supported on the CLE_κ carpet in the quantum disk. This measure conjecturally corresponds to the scaling limit of the uniform measure on a planar map with large faces, as studied for instance in [30], and it is therefore an interesting object to have at hand, if one tries to understand the scaling limit of such maps — see [5, 6] for results in this direction).

Theorem 1.3 (The natural LQG measure on the CLE carpet). *Consider a CLE_κ drawn on an independent $\sqrt{\kappa}$ -quantum disk, for $\kappa \in (8/3, 4)$. For any given open set O , define $N_\epsilon(O)$ to be the number of CLE_κ loops in O with LQG boundary length greater than ϵ . Then $\epsilon^{\alpha+1/2}N_\epsilon(O)$ converges in probability to a non-trivial finite random variable $\mathcal{Y}(O)$.*

This process \mathcal{Y} can therefore be interpreted as the *natural LQG measure* supported on the CLE carpet. The proof of this result is based on the following ideas: First, one can recall that “Kesten-Stigum”-type results on multiplicative cascades as developed in [5, 15] construct a “natural measure”

$\tilde{\mathcal{Y}}$ on the boundary of \mathcal{T} (i.e., on the CLE carpet) – motivated by the fact that it arises as the limit of the counting measure on some planar maps with large face, this measure is already called *the intrinsic area measure* in [5]. Then, one shows that this measure $\tilde{\mathcal{Y}}$ indeed corresponds to the quantity \mathcal{Y} described in the theorem, which in turn ensures that it is indeed a function of the CLE_κ and the LQG measure, and does not depend on the additional randomness that comes from the CPIs used to draw the exploration tree.

Note that when one applies the same ideas using $\tilde{\mathcal{T}}$ instead of \mathcal{T} (i.e., exploring the entire domain D instead of just the CLE carpet), one constructs the (usual) LQG area of the quantum surfaces using similar martingales.

1.2.3. *CLEs on quantum half-planes.* We will derive these results on CLE on a quantum disk as consequences of results for CLE on a quantum half-plane that we will now briefly describe. The results on a quantum half-plane somehow correspond to what happens in the quantum disk case when one zooms into the neighborhood of the starting point.

Here, one considers a quantum half-plane (also known as a particular quantum wedge) which is another quantum surface that can be naturally defined in a simply connected domain. This time, the choice of the harmonic function is such that the total quantum area of the domain and the total boundary length are infinite, but only in the neighborhood of one special boundary point (which is chosen to be ∞ when the domain is the upper half-plane). One then considers:

- A γ -quantum half plane, so that 0 is a “boundary-typical” point.
- An independent $\text{SLE}_\kappa(\kappa - 6)$ process from 0 to ∞ . The process traces some loops, that can be viewed as the CLE_κ loops encountered by the $\text{SLE}_{\kappa'}(\kappa' - 6)$ trunk (for $\kappa' = 16/\kappa$).

This CLE exploration can then be parameterized by the LQG-length of the CPI/trunk, and along the way, it will:

- Discover CLE_κ loops with quantum boundary lengths L_{t_i} at a countable random dense collection of times (t_i) . We can formally attach at once the entire loop to the CPI at this time t_i . When equipped with the LQG measure and with marked boundary point given by the point at which the loop is attached to the trunk, one obtains a quantum surface with one marked point.
- When the trunk bounces on the boundary of the remaining-to-be-explored region, it will disconnect some parts of \mathbf{H} from ∞ , by leaving them to its right or to its left. Again, the disconnected components (with marked point given by the disconnection point) is a quantum surface with one marked boundary point.

Theorem 1.4 (Exploration of a CLE on a quantum half-plane). *The three ordered families of quantum surfaces (cut out to the left, cut out to the right and inside the traced loops) by the quantum natural time of the trunk have the law of three independent Poisson point processes of quantum disks, defined under multiples a_l , a_- and a_+ of the same natural infinite measure on quantum disks, where $a_+ = a_-$ and $a_l = -2a_+ \cos(4\pi/\kappa)$.*

In other words, the CLE exploration on a quantum half-plane is related to the jumps of an $(4/\kappa)$ -stable process with asymmetry parameter $U = -\cos(4\pi/\kappa)$. This stable process is allowed to be negative, and can be thought off as the “variation” of the boundary length of the remaining-to-be explored region containing ∞ .

1.2.4. *Results for other CLE explorations.* We have so far only discussed the exploration of a CLE_κ by a totally asymmetric $\text{SLE}_\kappa(\kappa - 6)$ processes, that correspond to the fact that all CLE_κ loops are traced with the same orientation – or equivalently, lie on the same side of the trunk. In the percolation interpretation of the CPI, this corresponds to the fact that all the CLE_κ loops are declared to be closed for the considered percolation mechanism.

As explained and proved in [46, 49, 51], this is not the only possible natural way to proceed in order to explore a CLE in a conformally invariant way. One can choose a parameter $\beta \in [-1, 1]$ and decide at each time at which one discovers a CLE loop, to trace it clockwise with probability $1 - p := (1 - \beta)/2$ or counterclockwise with probability $p := (1 + \beta)/2$ (these choices are made independently for each loop). This defines the so-called $\text{SLE}_\kappa^\beta(\kappa - 6)$ processes – the previous totally asymmetric $\text{SLE}_\kappa(\kappa - 6)$ corresponds to the case $\beta = 1$. In the CPI percolation interpretation, it corresponds to the fact that loops can be closed or open for the considered percolation. As explained in [51], this procedure allows one to trace loops of a CLE_κ using $\text{SLE}_\kappa^\beta(\kappa - 6)$ processes. Also, it has been shown in [39] (among other things) that this exploration indeed traces a continuous path. The continuous path that one obtains when one erases all the CLE_κ -traced loops from this path is then a continuous curve, called the *trunk* of the $\text{SLE}_\kappa^\beta(\kappa - 6)$. When $\beta \in (-1, 1)$, some of the loops lie on the left-hand side of the trunk, and some of the loops lie to its right. It is intuitively clear (and this is made rigorous in [39]) that the respective proportion of loops attached to the two sides are $(1 + \beta)/2$ and $(1 - \beta)/2$.

One can therefore wonder what type of quantum surfaces will be cut out by this process when drawn on a quantum half-plane or a quantum disk. Note that this time, one will obtain four types of quantum surfaces because now, the CLE loops that one traces can be on the right-hand side of the trunk (the counterclockwise loops) or to the left-hand side of the trunk. As one could have somehow expected, it turns out that β only influences the left to right ratio of the positive jumps. In the case of the exploration of a quantum half-plane goes, the exact statement goes as follows:

Theorem 1.5 (Results for other explorations). *The four ordered families of quantum surfaces (cut out to the left, cut out to the right and inside the left loops, inside the right loops) by the quantum natural time of the trunk have the law of four independent Poisson point processes of quantum disks, respectively defined under a_- , a_+ , $a_{l,-}$ and $a_{l,+}$ times the measure on quantum disks, where $a_+ = a_-$, $a_{l,-} = (1 - p)a_l$ and $a_{l,+} = pa_l$ where $a_l = -2a_+ \cos(4\pi/\kappa)$.*

Actually, the knowledge of these four Poisson point processes allows one to reconstruct both the LQG-half-plane and the $\text{SLE}_\kappa^\beta(\kappa - 6)$ drawn on it. So, in a nutshell, the only difference with the totally asymmetric case is that each time one discovers a quantum disk that corresponds to a CLE loop, one tosses a $(1 + \beta)/2$ versus $(1 - \beta)/2$ coin to decide on which side of the trunk it will be. The similar result holds true for asymmetric explorations of quantum disks.

Theorem 1.5 makes it possible to complete the description of the loop-trunk of [39]. It is worthwhile to stress that this result does not involve any LQG, but that at present, we know of no way to derive it other than the one that we will give in this paper and that relies heavily on the interplay between CLE and LQG. Let us first remind the reader of one result from [39] about the law of the trunk of an $\text{SLE}_\kappa^\beta(\kappa - 6)$ process:

Theorem A (Theorem 7.4 from [39]). *For all $\kappa \in (8/3, 4)$ and $\beta \in [-1, 1]$, there exists $\rho' = \rho'(\beta, \kappa) \in [\kappa' - 6, 0]$ such that the law of the trunk of a $\text{SLE}_\kappa^\beta(\kappa - 6)$ process is a $\text{SLE}_{\kappa'}(\rho'; \kappa' - 6 - \rho')$ process for $\kappa' = 16/\kappa$.*

The fact that these $\text{SLE}_{\kappa'}(\rho'; \kappa' - 6 - \rho')$ processes for $\rho' \in [\kappa' - 6, 0]$ show up is not really surprising here: They are the natural target-invariant variants of $\text{SLE}_{\kappa'}(\rho')$ processes (in the same way as $\text{SLE}_{\kappa'}(\kappa' - 6)$ is the target-invariant variant of $\text{SLE}_{\kappa'}$ – see for instance [39] for a more detailed discussion). Recall also that in [39] the conditional law, given the trunk, of the collection of SLE_{κ} that are attached to the trunk is described. Except when $\beta \in \{-1, 0, 1\}$ that correspond to the totally asymmetric cases and to the symmetric case, we did not derive in [39] the values of $\rho'(\beta, \kappa)$. This following theorem provides the relation between ρ' and β :

Theorem 1.6 (The law of the trunk of $\text{SLE}_{\kappa}^{\beta}(\kappa - 6)$). *The value of $\rho' \in [\kappa' - 6, 0]$ in terms of $\beta \in [-1, 1]$ in Theorem A is determined by the relation (we write $1/0 = \infty$ so that this covers also the case $\beta = -1$):*

$$\frac{1 - \beta}{1 + \beta} = \frac{\sin(-\pi\rho'/2)}{\sin(-\pi(\kappa' - 6 - \rho')/2)}.$$

This therefore completes the full description of the loop-trunk decomposition of these asymmetric CLE exploration mechanisms.

The readers acquainted with subtleties of stable processes may find some similarities between this formula and that describing aspects of the ladder height processes of stable processes. This is not a coincidence, as we will actually derive Theorem 1.6 using those formulas.

1.3. Remarks, generalizations, outlook.

- (1) This paper will have a counterpart [38] that will describe the structures that one obtains when one draws $\text{CLE}_{\kappa'}$ -explorations (for $\kappa' \in (4, 8)$) on top of the corresponding quantum “half-planes” and “disks”. The results are formally quite similar to the ones of the present paper, but some of the arguments differ (to start with, the half-planes and disks will be of a different type).
- (2) The present paper (as well as [38]) lays the groundwork for stronger convergence results for scaling limits of discrete models to SLE on LQG to be made. In some sense, our results show that from the perspective of the continuum models that should appear in the scaling limit when one considers $O(N)$ models on well-chosen planar maps (or related models), the features that allowed physicists to use their *quantum gravity ideas* are indeed valid. It should therefore not be surprising that some of our formulas mirror results that appear in the study of some special planar maps, such as the ones arising in [10, 13, 5] (see also [11, 14] for further related results on the planar maps side). This can be explained by the fact that some of the discrete peeling type processes used in the study of planar maps should indeed give rise to these loops on trunk processes on independent LQG in the scaling limit.
- (3) To be more specific, the results of this article open the doors to using the QLE approach [37, 35, 36] to construct two particular metrics inside of the CLE carpet which correspond to the scaling limit of random planar maps with large faces determined by Le Gall and Miermont [30]. We plan to discuss this point in some more detail in [38].

Acknowledgements. JM was supported by ERC Starting Grant 804166 (SPRS). SS was supported by NSF award DMS-1712862. WW was supported by the SNF Grant 175505. He also acknowledges the hospitality of the University of Cambridge, where part of this work has been written.

2. BACKGROUND

2.1. Quantum wedges (thick and thin), half-planes and disks. Let us very briefly survey the definition of the quantum surfaces that we will be using in the present paper. The discussion that we give here will be somewhat informal because the precise definitions of these surfaces will not in fact be needed in this work. We refer the reader to [18, Section 1, Section 4] for a more detailed treatment.

One starting point is to consider the GFF in a simply connected domain with free boundary conditions. As this field turns out to be conformally invariant, it is sufficient to define it in \mathbf{H} , where it can be viewed as the Gaussian process h_F indexed by the space of bounded measurable functions with compact support and mean zero (w.r.t. Lebesgue measure), with covariance given by

$$\mathbf{E}[h_F(\phi)h_F(\psi)] = \int \phi(x)\psi(y) \left(\log \frac{1}{|x-y|} + \log \frac{1}{|x-\bar{y}|} \right) dx dy.$$

One way to interpret the fact that h_F is defined on the set of functions of zero mean, is that h_F is only defined “up to constants” (so in fact, the object that is defined and studied is the generalized function ∇h_F). One can of course also define a proper generalized function h_F and call it a GFF with free boundary conditions if $(h_F(\varphi))$ has the law described above (on the space of functions with zero mean).

For each choice of $\gamma \in (0, 2)$, one can almost surely associate to each such generalized function h_F a measure in the upper-half plane and a measure on the real line (i.e., that is thought of as the boundary of \mathbf{H}), for instance via a regularization procedure, that can be interpreted as the measures with densities $\exp(\gamma h_F)$ and $\exp(\gamma h_F/2)$ with respect to the area and length measure in the half-plane and the real line respectively. Such area and length measures can therefore also be defined for variants h of the free-boundary GFF, such that the law of h is locally absolutely continuous with respect to that of h_F (or to that of the sum of h_F with some random continuous function, or that of some randomly scaled version of it).

The quantum wedges are variants of the free boundary GFF involving two marked boundary points. It is at first sight convenient and natural, when working in \mathbf{H} , to take these two boundary points to be 0 and ∞ . Loosely speaking (we will make this more precise in a moment), the quantum wedges correspond to adding a constant times $\log|z|$ to the free boundary GFF. In this context, keeping in mind that it is the area measure that is conformally covariant, it appears however somewhat more natural to work in an bi-infinite strip (with marked boundary points at both ends of the strip) rather than in \mathbf{H} (so we just take the image of \mathbf{H} under the logarithmic map). In that setting, when h_F is a free-boundary GFF in the strip $\mathcal{S} = \mathbf{R} \times (0, \pi)$, we can consider $u_F(r)$ to be the mean-value of h_F on the vertical segment $(r, r + i\pi)$. This process $(u(r/2) - u(0))_{r \in \mathbf{R}}$ turns out to behave like a two-sided (i.e., bi-infinite) Brownian motion. Furthermore, if one defines the function u_F on the strip by $\tilde{u}_F(x + iy) = u(x)$, then the process $v_F := h_F - \tilde{u}_F$ is independent of u_F . In other words, adding a given function $f(\operatorname{Re}(z))$ amounts to twisting u_F only and to leave v_F unchanged.

In order to define the wedge variant, one essentially just has to choose u_F to be a Brownian motion with drift instead of a Brownian motion. However, it is well-known that a bit of care is needed when one defines a two-sided Brownian motion with drift¹ and because the free boundary GFF is defined only up to an additive constant.

¹One usual way to define a two-sided Brownian motion with drift is to declare that time 0 is the first time at which the Brownian motion with drift hits 0. Then, for positive times, the process is just a Brownian motion with drift, while on the negative side, it is Brownian motion with drift and conditioned not to hit the origin.

Let us briefly recall how to make sense of measures on one-dimensional drifted Brownian motion paths, starting from $-\infty$ at time $-\infty$. Note that here, we are somehow trying to make sense of measures on unparameterized paths. Since the Brownian motion's quadratic variation is constant, it is always possible to recover the difference between two times on the trajectory, but there is still one degree of freedom (for instance one can decide which point on the trajectory corresponds to time 0).

(i) When the drift a is positive, the natural measure on drifted Brownian paths is a probability measure, and the path will come from $-\infty$ (at time $-\infty$) and go to $+\infty$ (at time $+\infty$). This makes it possible to choose time 0 to be the first time at which the path hits 0. In that case, $(f(-t))_{t \geq 0}$ and $(f(t))_{t \geq 0}$ will be independent, the latter being just a Brownian motion with drift a , while the former will be a Brownian motion with drift a , but conditioned to never hit 0 (and there are several equivalent easy ways to make sense of this). An equivalent way to define this process is to use the fact that drifted Brownian motion can be viewed as a time-changed Bessel process. Here (with the positive drift), this means that one can start with a Bessel process Y of dimension δ greater than 2 (which is a process that starts from 0 at time 0, never hits 0 again, and tends to ∞ as time goes to ∞), and to view the drifted Brownian motion as a time-change of $\exp(Y)$ (the time-change ensures that the quadratic variation of the obtained process is constant, and the scaling property of the Bessel process then ensures that the obtained process behaves like a drifted Brownian motion). Then, again, one can choose where time 0 lies based on this drifted Brownian trajectory itself, for instance the first time at which it hits 0. For each positive value of a , one can then simply define the thick quantum wedge to be the surface obtained by adding the field v_F to this drifted Brownian motion. It defines an area measure in the bi-infinite strip, it has two special boundary points $-\infty$ and $+\infty$, and the area measure as well as the boundary length measure are finite in the neighborhood of $-\infty$ but infinite in the neighborhood of $+\infty$.

(ii) It is also natural to define measures on bi-infinite Brownian paths coming from $-\infty$ but with *negative* drift. This gives rise to infinite measures of Brownian-type paths that tend to $-\infty$ when time goes to $-\infty$ and also when time goes to $+\infty$. One can for instance define this as the appropriately renormalized limit when $M \rightarrow -\infty$ of the law P_M of Brownian motion with negative drift a started from M . For this limit to have a limit, one has to renormalize this probability measure P_M by (for instance) the probability that this paths hits 0. In other words, one is looking at the excursion measure away from $-\infty$ by the negatively drifted Brownian motion. The same alternative description via Bessel processes as above turns out to be handy as well. This time, the Bessel processes will have a dimension $\delta \in (0, 2)$ and the infinite measure that one starts with is simply the infinite measure on excursions away from 0 by this Bessel process. In any case, this leads to an infinite measure on surfaces with finite area and finite boundary length. The obtained measure is then self-similar in the sense that the measure on quantum surfaces that one obtains by multiplying the area measure by a given constant will be a multiple of the initial measure (the scaling factor can be read off from the drift of the Brownian motion or from the dimension of the Bessel process). This makes it then very natural to consider an ordered bi-infinite Poisson point process of quantum surfaces with intensity given by this infinite measure. The obtained infinite chain of quantum surfaces is then called a *thin quantum wedge* – to define it, one can therefore start with a bi-infinite Bessel process of dimension $\delta \in (0, 2)$ (that is equal to 0 at time 0) and defined on both positive and negative times.

The relation between the dimension δ of the Bessel process and the so-called weight W of the quantum wedge (one can view this formula as a definition of the weight W) is

$$(2.1) \quad \delta = 1 + \frac{2W}{\gamma^2}.$$

The threshold between thin and thick wedges is then at $W = \gamma^2/2$, corresponding to $\delta = 2$.

It is well-known that if one “conditions a Brownian motion with positive drift a to tend to $-\infty$ ” (it is easy to make rigorous sense of this conditioning), then one obtains a Brownian motion with the negative drift $-a$. This then corresponds to the well-known relation between Bessel processes of dimension δ and $4 - \delta$ (a Bessel process of dimension $\delta > 2$ conditioned to hit 0 will be a Bessel process of dimension $4 - \delta$). In terms of wedges, this corresponds to a natural “duality” relation between the thick quantum wedge of weight $W \in (\gamma^2/2, \gamma^2)$ and the beads of a thin quantum wedge of weight $W' = \gamma^2 - W$. We will come back to this later.

There are two special quantum surfaces that will play an important role here:

- For each $\gamma \in (0, 2)$, there is one very special thick quantum wedge for $W = 2$, that we will here call a quantum half-plane. Roughly speaking, this is the case where the boundary point $-\infty$ in the strip is not a particularly special boundary point of the quantum surface. For instance, when one samples such a quantum half-plane, and one chooses any fixed positive real b , one can define the point c on the bottom part of the boundary such that the boundary length of the half-line to the left of c is exactly equal to b . Then, one can consider a conformal map ϕ from the strip onto itself that maps c to $-\infty$ and keeps $+\infty$ unchanged (this map ϕ is then defined up to a horizontal translation). The special feature of the quantum half-plane is that the law of the obtained surface is again that of a quantum half-plane [47, 18].
- For each $\gamma \in (0, 2)$, among the measures on surfaces with finite area (beads of thin wedges, corresponding to excursions of Bessel processes), there is also one for which neither $-\infty$ nor $+\infty$ are particularly special boundary points – this is the case where $W = \gamma^2 - 2$, a bead of which we refer to as a quantum disk. Let us first define a simple operation on quantum surfaces as follows: Choose two boundary points c and c' independently according to the boundary length measure (renormalized to be a probability measure), and then consider a map ϕ from the strip onto itself, that maps c and c' onto $-\infty$ and $+\infty$ respectively (again this map is defined up to a horizontal translation). Then, when one applies this procedure, the measure on marked quantum surfaces induced by the Bessel excursions is invariant [18]. By scale invariance, it is possible to decompose this measure according to the total boundary length of the obtained surface, and to define a probability measure on quantum disks with a prescribed boundary length [18]. (We remark that at this stage, the wedge has a negative weight when $\gamma < \sqrt{2}$ – but we will anyway use only wedges with positive weight in the present paper).

Note that the weight $\gamma^2 - 2$ of the quantum disks and the weight 2 half-planes are related by the above-mentioned “duality relation” $W + W' = \gamma^2$.

If we parameterize a quantum wedge (or a bead of a thin quantum wedge) by \mathbf{H} and want to emphasize that the marked points are at 0 and ∞ , we will use the notation $(\mathbf{H}, h, 0, \infty)$. Similarly, if we parameterize it by \mathcal{S} and want to emphasize that the marked points are at $-\infty$ and $+\infty$, we will use the notation $(\mathcal{S}, h, -\infty, +\infty)$.

Remark 2.1. *Due to the LQG conformal covariance, there are several natural ways to actually define the quantum disk (i.e., to choose the domain D in which one defines it as well as the actual normalization one uses among all the conformal automorphisms of D). If one chooses the reference domain to be the infinite strip $\mathbf{R} \times (0, \pi)$ and chooses the embedding so that two boundary typical points are taken to $\pm\infty$, then one obtains the definition of the quantum disk developed in [47, 18]. If one alternatively chooses to fix the embedding using three points, then the definition one obtains is as described in [27]. A proof of the equivalence between these definitions can be found in [12].*

This mirrors the similar story for the definitions of LQG spheres, where the approaches developed in [47, 18] and in [16] were proven to be equivalent in [1]. In the present article, we will use the version of the disk with two marked points as it is amenable to SLE techniques (the two points corresponding to the seed and target of the SLE).

2.2. SLE explorations of quantum surfaces. We will now recall some of the basic welding operations which are proved in [18] and which we will make use of later in the proofs of our main results. The first result is regarding the case of welding quantum wedges along their boundaries (or equivalently cutting with an independent SLE_κ -type curve):

Theorem B (Theorems 1.2 and 1.4 from [18]). *(i) Let $\mathcal{W} = (\mathbf{H}, h, 0, \infty)$ be a thick quantum wedge of weight W . Fix $\rho_1, \rho_2 > -2$ with $\rho_1 + \rho_2 + 4 = W$. Let η be an independent $\text{SLE}_\kappa(\rho_1; \rho_2)$ process in \mathbf{H} from 0 to ∞ . If we let \mathcal{W}_1 (resp. \mathcal{W}_2) be the quantum surface which is parameterized by the part of $\mathbf{H} \setminus \eta$ which is to the left (resp. right) of η , then $\mathcal{W}_1, \mathcal{W}_2$ are independent quantum wedges with weights $W_1 = \rho_1 + 2$ and $W_2 = \rho_2 + 2$. Furthermore, η and \mathcal{W} are both almost surely determined by \mathcal{W}_1 and \mathcal{W}_2 .*

(ii) The same result holds true if \mathcal{W} is a thin quantum wedge of weight W except that η is defined to be a concatenation of independent $\text{SLE}_\kappa(\rho_1; \rho_2)$ processes, one for each bead of \mathcal{W} .

We will in fact mostly be using statement (i) in the case where $\rho_2 = 0$, in which case \mathcal{W}_2 is a quantum half-plane. Note that for statement (ii) to hold for a thin wedge, the formula $\rho_1 + \rho_2 + 4 = W$ will require ρ_1 and ρ_2 to be negative.

The second result that we will restate is the analogous result for $\text{SLE}_{\kappa'}(\rho_1; \rho_2)$ processes for $\kappa' \in (4, 8)$:

Theorem C (Theorem 1.17 from [18]). *Assume that $\gamma \in (\sqrt{2}, 2)$. Fix $\rho_1, \rho_2 \geq \kappa'/2 - 4$, let $W_i = \gamma^2 - 2 + (\gamma^2 \rho_i/4)$ for $i = 1, 2$, and $W = W_1 + W_2 + 2 - \gamma^2/2$. Suppose that $\mathcal{W} = (\mathbf{H}, h, 0, \infty)$ is a quantum wedge of weight W . Let η' be an independent $\text{SLE}_{\kappa'}(\rho_1; \rho_2)$ process in \mathbf{H} from 0 to ∞ . Then the quantum surface parameterized by the components which are to the left (resp. right) of η' is a quantum wedge of weight W_1 (resp. W_2) and the quantum surfaces parameterized by the components which are completely surrounded by η' are all quantum disks given their boundary lengths.*

This makes it in particular quite natural to draw an $\text{SLE}_{\kappa'}$ on top of a quantum wedge of weight $3\gamma^2/2 - 2$. In that case, let us recall the boundary length evolution description:

Assume that $\gamma \in (\sqrt{2}, 2)$. Suppose that $\mathcal{W} = (\mathbf{H}, h, 0, \infty)$ is a quantum wedge of weight $W = 3\gamma^2/2 - 2$. Let η' be an independent $\text{SLE}_{\kappa'}$ in \mathbf{H} from 0 to ∞ . We parameterize η' by its quantum length (induced by \mathcal{W}). For each $t \geq 0$, we let L_t (resp. R_t) denote the change in the left (resp. right) side of the outer boundary of $\mathbf{H} \setminus \eta'([0, t])$ relative to time 0 (i.e., $L_0 = R_0 = 0$). Note that each downward jump of L (resp. R) corresponds to a component separated from ∞ by η' at the corresponding time and the length of the jump gives the quantum boundary length of the disconnected region. Recall from (1.1) that $\alpha = 4/\kappa = \kappa'/4$.

Theorem D (Theorem 1.18 and Corollary 1.19 from [18]). *(i) The processes L and R are independent α -stable Lévy processes. This describes in particular the law of the jumps. Moreover, the quantum surfaces parameterized by the components are conditionally independent quantum disks given their boundary lengths.*

(ii) Furthermore, for each $t \geq 0$, we can consider the unbounded connected component H_t of the complement of $\eta[0, t]$, and view this as a quantum surface. We can also consider the

complement K_t of H_t in \mathbf{H} , and also view it as a quantum surface. Then H_t is a quantum wedge of weight $3\gamma^2/2 - 2$, that is independent of the quantum surface K_t decorated by η' up to time t .

- (iii) Finally, \mathcal{W} and η' are a.s. determined by the boundary length processes L, R and corresponding collection of quantum disks, each marked by the first point on their boundary visited by η' .

2.3. The loop-trunk decomposition of $\text{SLE}_\kappa^\beta(\kappa - 6)$. The loop-trunk decomposition of the $\text{SLE}_\kappa^\beta(\kappa - 6)$ processes, which Theorem A is part of, provides the description of the conditional law of the CLE loops encountered by the process, given its trunk, in terms of *boundary conformal loop ensembles* (BCLE) introduced in [39].

We here review the results that will be used in the present work: Suppose that $\kappa \in (8/3, 4)$ and that $\beta = 1$. Then, it turns out that the $\text{SLE}_\kappa(\kappa - 6)$ process (from 0 to ∞ in \mathbf{H}) is a continuous curve η . Each of the excursions away from 0 made by the Bessel process used to define this $\text{SLE}_\kappa(\kappa - 6)$ process corresponds to a closed simple loop made by η . If one excises all these loops from η , one obtains a (non-simple) curve η' from 0 to ∞ , called the trunk of η . The law of this trunk is an $\text{SLE}_{\kappa'}(\kappa' - 6)$. Suppose now that τ' is a finite stopping time for the trunk (this stopping time can use some additional randomness that does not come from η , we will typically later take τ' to be the first time at which the LQG-length of η' reaches a certain level). This time τ' almost surely corresponds to a single time τ for η .

So, in this first description, we have a concrete description of $\eta[0, \tau]$: Run the $\text{SLE}_\kappa(\kappa - 6)$ until time at which its trunk time is τ' . One main result of [39] is the following alternative description: Run first the trunk alone until time τ' , and then use the description of the conditional law of η given $\eta'[0, \tau']$ that is given in [39] in terms of boundary conformal loop ensembles. One consequence of this description is the following:

Proposition E ([39]). *The conditional law of the unbounded connected component of $\mathbf{H} \setminus \eta[0, \tau]$ given $\eta'[0, \tau']$ can be obtained by running an $\text{SLE}_\kappa(3\kappa/2 - 6)$ process η'' from the right-most intersection point x of $\eta'_{[0, \tau']}$ with the real line, to $\eta'_{\tau'}$ (with marked point at its starting point). This component is distributed as the unbounded connected component of $\mathbf{H} \setminus (\eta'[0, \tau'] \cup \eta'')$.*

Recall that $\text{SLE}_\kappa(\rho)$ processes for $\rho > -2$ are reversible (see [34]), and also that an $\text{SLE}_\kappa(\rho)$ process from a to b with marked point at c can be viewed as an $\text{SLE}_\kappa(\kappa - 6 - \rho)$ process from a to c with marked point at b – which leads to a number of equivalent descriptions of this conditional law of η'' (for instance as an $\text{SLE}_\kappa(-\kappa/2)$ process).

In Proposition E, each excursion of η'' away from the trunk η' corresponds to a portion of the same simple CLE_κ loop traced by the $\text{SLE}_\kappa(\kappa - 6)$ process η . To finish this loop, it is shown in [39] that one needs to draw an $\text{SLE}_\kappa(-\kappa/2)$ η''' in the “pocket” in between this excursion and η' . To then find the loops of η squeezed in between η' and η''' , one can iterate the procedure, by drawing alternatively $\text{SLE}_\kappa(3\kappa/2 - 6)$ and $\text{SLE}_\kappa(-\kappa/2)$ processes.

2.4. An instance of imaginary geometry coupling. In the derivation of the previously stated results, the “imaginary geometry” coupling of several SLE-type curves with an auxiliary GFF was instrumental. A particular instance of these flow-line/counterflow line interaction will be the following (which follows from the statements in [33]):

Consider the upper half-plane \mathbf{H} , and a GFF with boundary conditions $\lambda' = \pi/\sqrt{\kappa'}$ on \mathbf{R}_+ and $-\lambda'$ on \mathbf{R}_- . One can then define the “counterflow-line” of this GFF starting at 0 aiming ∞ – this is an

$\text{SLE}_{\kappa'}$ curve η' from 0 to ∞ . It is also possible, for the same GFF, to consider a “flow line” from ∞ to 0, of appropriate angle, so that this curve F is an $\text{SLE}_{\kappa}(3\kappa/2 - 6)$ from ∞ to 0, see Figure 4. This is a simple curve that intersects the positive half-axis many times, but not the negative half-axis. We can define the infinite connected component H of the complement of F . Then, for this coupling, a feature that will be very useful in our proofs is that *the conditional law of η' given F is that of an $\text{SLE}_{\kappa'}(\kappa' - 6)$ in H .*

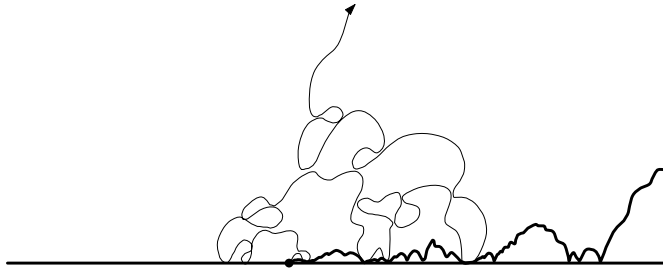


FIGURE 4. The coupling of the $\text{SLE}_{\kappa'}(\kappa' - 6)$ with the $\text{SLE}_{\kappa}(3\kappa/2 - 6)$

A variant of the previous statement occurs if one considers η' up to some stopping time τ' (that possibly involves additional randomness). Indeed (and this is of course related to the conformal Markov property of η'), up to the imaginary geometry change of coordinates formula described in [33], the GFF in the unbounded connected component H' of the complement of $\eta'[0, \tau']$ has boundary conditions λ' and $-\lambda'$ on the two sides of $\eta'_{\tau'}$. One can therefore consider in H' the flow line \tilde{F} from ∞ to $\eta'_{\tau'}$, of the same angle as F , see Figure 5. This flow-line will then coincide with F until the first point at which it touches $\eta'[0, \tau']$, and the remaining part of \tilde{F} (that we call F' and will play a key role in the proof of Proposition 3.1) will be an $\text{SLE}_{\kappa}(3\kappa/2 - 6)$ from x to $\eta'_{\tau'}$ in the remaining domain.



FIGURE 5. The variant at finite time of the coupling. We will use in the sequel that the latter part of the flow-line can be viewed as the outer boundary of an $\text{SLE}_{\kappa}(\kappa - 6)$ process as on the bottom figure.)

3. EXPLORING CLEs ON QUANTUM HALF-PLANES

Throughout this section, we will consider $\gamma \in (\sqrt{8/3}, 2)$ and $\kappa = \gamma^2 \in (8/3, 4)$. We will also assume that $\kappa' = 16/\kappa$ and $\alpha = 4/\kappa = \kappa'/4$ as in (1.1). We will begin in Section 3.1 by showing that the law of the quantum half-plane is invariant under the operation of cutting along an independent $\text{SLE}_\kappa(\kappa - 6)$ process up to a given amount of LQG length for its trunk, and that the collection of quantum surfaces that are cut off to the left of the trunk form a Poisson point process of quantum disks. We emphasize that in this section, we do not yet prove that the surfaces that are surrounded by CLE loops or cut out to the right of the trunk are also quantum disks (we will only describe their boundary lengths). We then deduce from this all the relations between CLE explorations on independent LQG surfaces (in the infinite volume setting) and Lévy processes and trees. Next, in Section 3.2, we will derive the corresponding results for $\text{SLE}_\kappa^\beta(\kappa - 6)$ processes for all β and the formula that describes the law of the trunk of these $\text{SLE}_\kappa^\beta(\kappa - 6)$ processes (Theorem 1.6). Finally, in Section 3.3 we will prove that all of the surfaces cut off by an $\text{SLE}_\kappa^\beta(\kappa - 6)$ are quantum disks given their boundary lengths.

3.1. Stationarity. Consider a quantum half-plane $\mathcal{W} = (\mathbf{H}, h, 0, \infty)$. In the sequel, when O is an open subset of \mathbf{H} (with some marked points), we will always use on O the area measure given by \mathcal{W} when we refer to O as a quantum surface.

Consider a totally asymmetric $\text{SLE}_\kappa(\kappa - 6)$ process η in \mathbf{H} from 0 to ∞ , with $\kappa = \gamma^2 \in (8/3, 4)$. Along the way, this process cuts a countable family of quantum surfaces away from ∞ . This happens (i) when η closes a CLE loop, (ii) when the trunk hits \mathbf{R} or a point that had already been visited by η (note that only countably many of such double-points correspond to times at which a surface is actually cut out from infinity – for example, in the set of times at which the trunk hits \mathbf{R} , only the times that are isolated from the left will satisfy this property). Those special double points of η will correspond to one of the countably many times at which η splits the remaining to be discovered domain into two parts. It can disconnect a domain to its right or to its left. We denote by \mathcal{F}_t the filtration generated by these three collections of quantum surfaces (corresponding to loops, cut out by the trunk to its left and cut out by the trunk to its right) up to time t . We view these quantum surfaces as *marked* quantum surfaces with one or two marked boundary points: When it corresponds to a CLE loop, there is only one marked point, which is the position of the tip of the trunk at this disconnection time. When it corresponds to a domain cut out by the trunk which does not intersect \mathbf{R} , one also has one marked point corresponding to the disconnection time. Finally, when it corresponds to a domain cut out by the trunk which intersects \mathbf{R} , one has two marked points corresponding to the first and last boundary point visited by η .

Since the trunk of η is an $\text{SLE}_{\kappa'}(\kappa' - 6)$ process independent of \mathcal{W} , it is possible to define its LQG-quantum length. We denote by $\tau' = \tau'_t$ the first time at which this LQG length reaches t , and we denote by $\tau = \tau_t$ the corresponding time for η . The σ -field \mathcal{F}_τ therefore contains the information about all the quantum surfaces that have been cut out by $\eta[0, \tau]$ from ∞ . We define $\mathcal{G}_t := \mathcal{F}_{\tau_t}$.

The first main key result is the following:

Proposition 3.1. *(i) For each $t \geq 0$, the quantum surface parameterized by the unbounded component of $\mathbf{H} \setminus \eta([0, \tau_t])$ with marked points $\eta(\tau)$ and ∞ is a quantum half-plane, which is independent of \mathcal{G}_t .*
(ii) Let $(S_{t_i}^-)_{t_i > 0}$ denote the point process of quantum surfaces that are cut out to the left of the trunk of η . (In other words, $S_{t_i}^-$ is not empty if exactly at τ_{t_i} , the trunk cuts out a bounded

connected component O_{t_i} from ∞ to its left.) Then the process $(S_{t_i}^-)_{t_i > 0}$ is a Poisson point process of marked quantum disks (with intensity measure given by a constant a_- times the infinite measure on quantum disks).

- (iii) Let L_t (resp. R_t) denote the change in the boundary length of the left (resp. right) side of the unbounded component of $\mathbf{H} \setminus \eta([0, \tau_t])$ relative to time 0. Then L_t and R_t are independent α -stable Lévy processes.

Proof. It is convenient to start with a quantum wedge $\widetilde{\mathcal{W}} = (\mathbf{H}, \tilde{h}, 0, \infty)$ of weight $3\gamma^2/2 - 2$, which is “wider” than the quantum half-plane, and to view the quantum half-plane as a subset of this quantum wedge. More precisely, Theorem B implies that if one draws an independent $\text{SLE}_{\kappa}(3\kappa/2 - 6)$ from ∞ to 0 (with marked point at ∞ to start with) that we call F , then the unbounded connected component of the complement of F will be a quantum half-plane (that is independent of the quantum surfaces with bounded area that are cut out from ∞ by the path), see Figure 6.

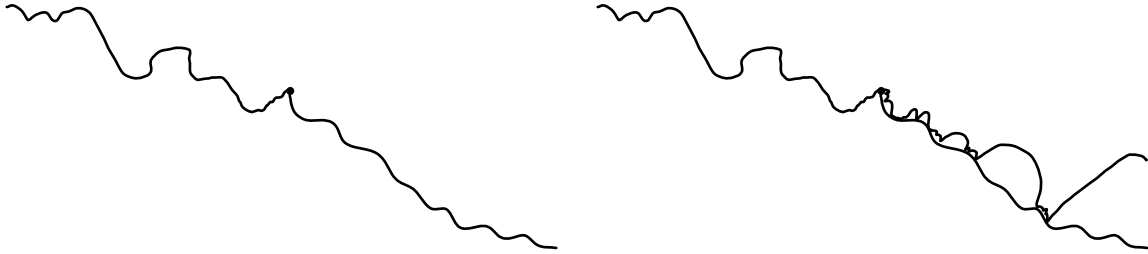


FIGURE 6. Symbolic sketch: The wedge (above the curve), the $\text{SLE}_{\kappa}(3\kappa/2 - 6)$ and the half-plane (above the curves)

We now consider η' to be an independent $\text{SLE}_{\kappa'}$ from 0 to ∞ in \mathbf{H} . We couple η' with an $\text{SLE}_{\kappa}(3\kappa/2 - 6)$ process F from ∞ to 0 as described in Section 2.4. We let H be the unbounded connected component of the complement of F . Recall also the definitions of x , \tilde{F} and F' from Section 2.4.

Then, using Theorem C on the one hand, and the properties of the coupling of F with η' , we see that the triplet $(H, 0, \infty)$ equipped with the area measure from $\widetilde{\mathcal{W}}$ is a quantum half-plane, and that conditionally on F , the process η' is an $\text{SLE}_{\kappa'}(\kappa' - 6)$ from 0 to ∞ in H' . So, we can use η' in H as a model for our $\text{SLE}_{\kappa'}(\kappa' - 6)$ on an independent quantum half-plane, see Figure 7.

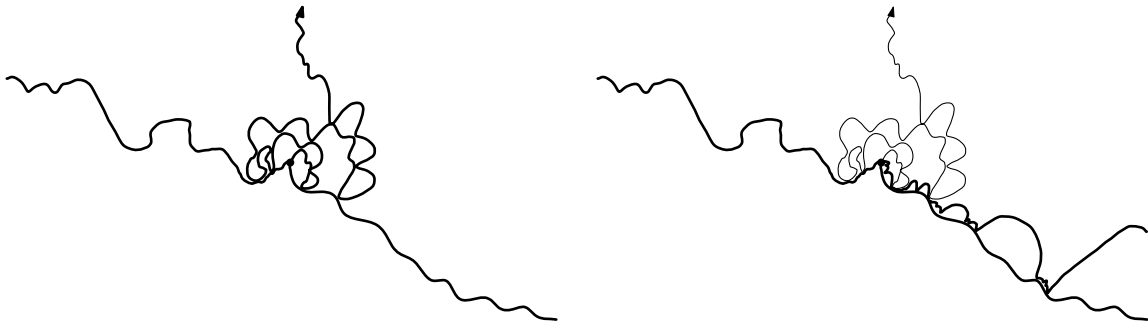


FIGURE 7. Symbolic sketch: The $\text{SLE}_{\kappa'}$, viewed in the wedge – the complement is still a wedge. The curve viewed in the half-plane is an $\text{SLE}_{\kappa'}(\kappa' - 6)$

The crucial point now is that the conditional law of the outer boundary of $\eta[0, \tau]$ is given by an additional $\text{SLE}_\kappa(3\kappa/2 - 6)$ from x to $\eta'_{\tau'}$ in $H' \setminus \eta'[0, \tau']$ – which happens to be the same as the conditional law of F' . We can therefore choose our coupling in such a way that this outer boundary is exactly F' .

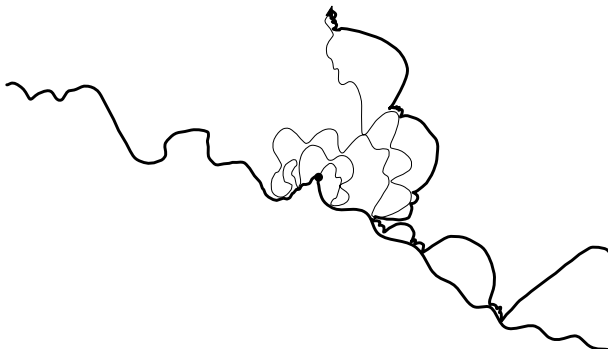


FIGURE 8. Symbolic sketch: Creating a half-plane by running the $\text{SLE}_\kappa(3\kappa/2 - 6)$ in the wedge of the left of Figure 7. Its latter part can be viewed as the right boundary of the $\text{SLE}_\kappa(\kappa - 6)$ that η' is the trunk of.

Hence, the quantum surface parameterized by the unbounded component of $\mathbf{H} \setminus \eta([0, \tau])$ with marked points $\eta(\tau)$ and ∞ can be realized as follows: In the unbounded connected component H'' of $\mathbf{H} \setminus \eta'[0, \tau']$, draw an independent $\text{SLE}_\kappa(3\kappa/2 - 6)$ from ∞ to $\eta'_{\tau'}$ and consider the infinite connected component of its complement, with marked points $\eta'_{\tau'}$ and ∞ .

But we know that H'' with marked points $\eta'(\tau')$ and ∞ is a quantum wedge of weight $3\gamma^2/2 - 2$, that is independent of all the quantum surfaces cut out of η' up to this time. So, when one draws this $\text{SLE}_\kappa(3\kappa/2 - 6)$ as in Figure 8, one obtains a quantum half-plane, which shows the first statement.

Since by construction, the process $(S_{t_i}^-)_{t_i > 0}$ is the same as that cut out on its left by the SLE_κ process in the quantum wedge $\widetilde{\mathcal{W}}$, and we know by Theorem D that this is a Poisson point process of marked quantum disks, so that the Poisson point process of the corresponding boundary lengths has an intensity $a_- dl/l^{\alpha+1}$.

The first assertion of the proposition implies that L_t and R_t have stationary independent increments and are therefore Lévy processes. Scaling considerations analogous to the second assertion of the proposition imply that L_t and R_t are α -stable. That L_t and R_t are independent follows because a.s. the two processes do not have a simultaneous jump. \square

If we now define by S^+ and S^ℓ to be the two point processes of quantum surfaces cut out to the right of the trunk and by a CLE loop in exactly the same way as S^- , the stationarity and independence statement from Proposition 3.1 show that the law of (S^+, S^-, S^ℓ) after time τ_t is independent of the point processes of surfaces that have appeared before time t . Furthermore, we note that two different quantum surfaces can never appear at the same time on the trunk (because of the continuity of the trunk and of the Markovian property of $\text{SLE}_\kappa(\kappa - 6)$ when it is on the trunk). It therefore follows that the three processes S^- , S^+ and S^ℓ are independent Poisson point processes of marked quantum surfaces. We are not yet going to show that S^- and S^ℓ are also Poisson point processes of quantum disks, but we will now derive the corresponding result about their boundary lengths. More precisely, let Λ^+ , Λ^- and Λ^ℓ denote the three point processes consisting of the quantum boundary lengths of the surfaces appearing in S^+ , S^- and S^ℓ .

Corollary 3.2. *The intensities of the Poisson point processes Λ^+ , Λ^- and Λ^ℓ are all multiples of the measure $dl/l^{\alpha+1}$.*

Proof. We have already proved the result for Λ^- in Proposition 3.1. By the scaling property of the quantum half-plane (scaling both space and the area measure also defines a quantum half-plane), if m^+ and m^- denote the intensity measures of Λ^+ and Λ^ℓ , we get that the ratio $m^+[x, \infty)/m^-[x, \infty)$ does not depend on x (and the similar result for the intensity measure of Λ^ℓ), from which the corollary follows. \square

Let us denote the multiplicative constants for the three intensities by a_- , a_+ and a . We denote by U the ratio $a/(a_- + a_+)$. We will see in the next section that in fact $a_- = a_+$ and $U = -\cos(\pi\alpha)$.

3.2. Densities of jumps for all CLE explorations. Suppose that $\mathcal{W} = (\mathbf{H}, h, 0, \infty)$ is a quantum half-plane. For $\beta \in [-1, 1]$, we let η be an $\text{SLE}_\kappa^\beta(\kappa - 6)$ process on \mathbf{H} from 0 to ∞ . Suppose that $\epsilon > 0$ is fixed. We can approximate the law of η by that of a process η^ϵ as follows. Let $p = (1 + \beta)/2$. One tosses first a p v.s. $1 - p$ coin to decide if up to the first time at which the quantum length of its trunk is ϵ , the process η evolves as an $\text{SLE}_\kappa^1(\kappa - 6)$ process or an $\text{SLE}_\kappa^{-1}(\kappa - 6)$ process. Then, one tosses another independent coin to decide about the behavior of η up to the time at which the trunk has quantum length 2ϵ and so on. When $\epsilon \rightarrow 0$, the process η^ϵ converges to η in distribution, and in fact, it is possible to couple η^ϵ with η by choosing the coin tosses appropriately.

We now look at the Poisson point process of quantum surfaces that are cut out by the $\text{SLE}_\kappa^\beta(\kappa - 6)$. There are now four point processes: Those cut out by the trunk to its left, those cut out by the trunk to its right, those corresponding to loops that lie to the left of the trunk, and those that correspond to loops that lie to the right of the trunk.

The previous limiting description (as $\epsilon \rightarrow 0$ of the side-swapping process), shows immediately, that the Poisson point processes of boundary lengths of these quantum surfaces have intensities that are multiples of $dl/l^{\alpha+1}$, where the multiplicative constants are respectively $pa_- + (1 - p)a_+$, $pa_+ + (1 - p)a_-$, $(1 - p)a$ and pa .

The following paragraphs are now devoted to the proof of Theorem 1.6 (the law of the trunk of η) and it will also contain a proof of the fact that $U = -\cos(\pi\alpha)$ and that $a_- = a_+$.

Recall the statement of Theorem A that for each value of $\kappa \in (8/3, 4)$, $\beta \in [-1, 1]$, there exists ρ' such that the trunk η' of η is an $\text{SLE}_{\kappa'}(\rho'; \kappa' - 6 - \rho')$ process. Apart in the special cases $\beta = -1, 0, 1$, we do not know yet what the value of ρ' is (but we will now determine it).

When we draw η in \mathbf{H} , we know that the points at which it intersects \mathbf{R} are exactly the same points at which the trunk η' intersects \mathbf{R} . If we endow the half-plane with a quantum half-plane structure as before, then we will be able to interpret the quantum lengths intervals on the real in between these hitting points in two different ways – one in terms of a Lévy process related to η' (and therefore of η) and one in terms of a Lévy process related to η (and therefore to β).

Let L (resp. R) denote the process of left (resp. right) boundary length variation (when parameterized by the LQG length of the trunk) of η . We proved in Proposition 3.1 that L and R are independent α -stable Lévy processes in the case that $\beta = 1$. The same limiting argument described above gives the same statement for all $\beta \in [-1, 1]$. Such processes have been studied quite extensively (see [3] and the references therein). In particular, one has a complete description of the Poisson point process of jumps of their running infimum. These jumps correspond exactly to the quantum lengths of intervals in between the points at which η' hits \mathbf{R}_- and \mathbf{R}_+ .

By [3, Chapter VIII, Lemma 1] we know that the Lévy measure for these jumps (corresponding to the “ladder height process”) for L is a constant times $x^{-\alpha P_L - 1} dx$ where dx denotes the Lebesgue measure on \mathbf{R}_+ and P_L denotes the so-called positivity parameter of L , that is related to the ratio $U_L = U_L(\beta)$ between the intensity of positive versus negative jumps of L by the formula

$$U_L = \frac{\sin(\pi\alpha(1 - P_L))}{\sin(\pi\alpha P_L)}.$$

One has of course the same formula relating P_R and U_R .

But our LQG description allows one to get another expression for this exponent. We consider this time only the connected components of the complement of η' that intersect \mathbf{R}_- and \mathbf{R}_+ , respectively. By Theorem C, the collection of these LQG surfaces form quantum wedges \mathcal{W}_L and \mathcal{W}_R of respective weights

$$W_L = \kappa - 2 + \kappa\rho'/4, \quad \text{and} \quad W_R = \kappa - 2 + \kappa(\kappa' - 6 - \rho')/4.$$

Recall from (2.1) that a quantum wedge of weight W is encoded by a Bessel process of dimension $1 + 2W/\gamma^2$. The dimensions of the Bessel processes which encode \mathcal{W}_L , \mathcal{W}_R are therefore

$$\delta_L := 3 - \alpha + \frac{\rho'}{2} \quad \text{and} \quad \delta_R := \alpha - \frac{\rho'}{2}.$$

Recall that each excursion of the encoding Bessel process corresponds to a bead of the thin quantum wedge. We note that the Lévy measure of the maxima of the excursion of a Bessel process of dimension δ is a constant times $x^{\delta-3} dx$, and that the boundary length of the bead is a function of this excursion that scales like this maximum. It therefore follows that the Lévy measure of the boundary lengths of the beads is also a constant times $x^{\delta-3} dx$. By independence of the beads, we similarly get that the lengths of the boundary lengths of the intervals in between the hitting points of η' on \mathbf{R} have the same scaling behavior.

Identifying $\delta_L - 3$ with $-\alpha P_L - 1$, we get $\alpha P_L = \alpha - (\rho'/2) - 1$ and

$$U_L(\beta) = \frac{\sin(-\pi\rho'/2)}{\sin(\pi(-\alpha + \rho'/2))}$$

By symmetry, one obtains a similar expression for U_R replacing ρ' by $\kappa' - 6 - \rho'$.

We can note that by symmetry, in the case where $\beta = 0$ (i.e., symmetric exploration of the CLE), one knows that $\rho' = \kappa' - 6 - \rho'$ so that

$$\rho' = \kappa'/2 - 3 = 2\alpha - 3.$$

In this case, the formula for ratio between the intensities of upwards versus downwards jumps of both R and L (which is equal to $a/(a_+ + a_-)$) turns out to be

$$U_L(0) = U_R(0) = \frac{\sin(\pi(\alpha - 3/2))}{\sin(-3\pi/2)} = -\cos(\pi\alpha).$$

When $\beta = -1$, we also know that $\rho' = 0$. Plugging this into the previous formula, we see that in this case the ratio between the intensities of upwards versus downwards jumps of L (which is equal to a/a_-) is

$$U_L(-1) = -\frac{\sin(2\pi\alpha)}{\sin(\pi\alpha)} = -2\cos(\pi\alpha).$$

We therefore conclude that $a_- = a_+$ and that $a/(a_+ + a_-) = -\cos(\pi\alpha)$.

For general β , this then shows that $U_R(\beta)/U_L(\beta)$ is equal to the ratio between the intensities of the positive jumps of R and L , which is equal to $(1-p)a/(1+p)a = (1-\beta)/(1+\beta)$; we therefore get that

$$\frac{1-\beta}{1+\beta} = \frac{\sin(-\pi\rho'/2)}{\sin(-\pi(\kappa'-6-\rho')/2)}$$

which concludes the proof of Theorem 1.6 (note that we kept the minus signs in the two sin expressions because ρ' and $\kappa'-6-\rho'$ are negative).

At this point, the only missing item to complete the proofs of Theorems 1.4 and 1.5 is the fact that all the quantum surfaces that are cut out are independent quantum disks given their boundary length (which then implies that S^+ and S^ℓ are point processes of quantum disks), which is what we explain in the next section.

3.3. All cut-out surfaces are quantum disks. Our goal is now to explain why S^ℓ and S^+ are point processes of quantum disks. By the previous side-swapping construction of $\text{SLE}_\kappa^\beta(\kappa-6)$, we see that it is sufficient to prove this for the totally asymmetric $\text{SLE}_\kappa(\kappa-6)$ process η . We draw η on an independent quantum half-plane $(\mathbf{H}, h, 0, \infty)$ as in Section 3.1 and denote its trunk by η' .

We know by Theorem C that η' slices the quantum half plane into three independent quantum wedges of respective weights γ^2-2 , $2-\gamma^2/2$ and $2-\gamma^2/2$, corresponding respectively to the surfaces that are cut out to the left of the trunk (with boundaries intersecting \mathbf{R}_-), the surfaces between the left and right boundaries of the trunk, and the surfaces that lie to the right of the trunk (with boundaries that intersect

R_+).

The beads of the first quantum wedge (to the left of the trunk, components touching \mathbf{R}_-) are quantum disks, which is of course consistent with the fact that the process S^- is a point process of quantum disks (mind however that not all surfaces of S^- will be part of this wedge – they will form a “forested wedge” in the terminology of [18]). Let us now focus on the latter (“rightmost”) quantum wedge \mathcal{V} with weight $2-\gamma^2/2$. (Note that $2-\gamma^2/2$ is smaller than γ^2-2 because $\kappa > 8/3$, and that \mathcal{V} is in fact the “dual” of the thick wedge of weight $3\gamma^2/2-2$ that we used before). By the loop-trunk decomposition of η , we know the “right boundary” η'' of η , will consist of the concatenation of $\text{SLE}_\kappa(3\kappa/2-6)$ processes (one independent one in each of the beads of the wedge \mathcal{V} , from one marked point of the wedge to the other one). We will deduce that S^+ and S^- are Poisson point processes of quantum disks from the following facts:

Lemma 3.3. *(i) Consider a bead of a quantum wedge of weight $W = 2 - \gamma^2/2$. Draw an independent $\text{SLE}_\kappa(3\kappa/2-6)$ from one of its marked points to the other one. Then, conditionally on its boundary length, the surface cut out to the right of the path is a quantum disk, and conditionally on their boundary lengths, the surfaces cut out to its left are beads of a quantum wedge of weight $W' = 3\gamma^2/2 - 4$.*

(ii) Consider a bead of a quantum wedge of weight $W' = 3\gamma^2/2 - 4$. Draw an independent $\text{SLE}_\kappa(-\kappa/2)$ from one of its marked points to the other one. Then, conditionally on its boundary length, the surface cut out to the right of the path is a quantum disk, and conditionally on their boundary lengths, the surfaces cut out to its left are beads of a quantum wedge of weight $W = 2 - \gamma^2/2$.

The two parts of Lemma 3.3 can be viewed as the “finite-volume” counterpart of the following two special cases of Theorem B:

- An $\text{SLE}_\kappa(3\kappa/2 - 6)$ cuts a wedge of weight $3\gamma^2/2 - 2$ (the dual of W) into a half-plane and a wedge of weight $W' = 3\gamma^2/2 - 4$.
- An $\text{SLE}_\kappa(-\kappa/2)$ cuts a wedge of weight $4 - \gamma^2/2$ (the dual of W') into a half-plane and a wedge of weight $W = 2 - \gamma^2/2$.

As we will explain in the appendix devoted to the proof of Lemma 3.3, it is part of a much larger family of results, but we choose to here highlight just those two for presentation purposes.

Remark 3.4. *If we would have started with an entire thin quantum wedge in Lemma 3.3 and traced the $\text{SLE}_\kappa(\rho)$ in each of the beads, then it is not possible to apply the thin-wedge part of Theorem B because of the condition that W_1 and W_2 have to be positive (i.e., a thin wedge of weight $\gamma^2 - 2$ can not be contained in a thin wedge of weight $2 - \gamma^2/2$ because we are in the regime where $\kappa > 8/3$).*

The first statement of Lemma 3.3 shows that all the quantum surfaces cut out to the right of the trunk η' by η and whose boundaries intersect \mathbf{R} are independent quantum disks when conditioned on their respective boundary lengths (i.e., resampling each one does not change the law of this process). We should keep in mind that (just as for S^-), most of the quantum surfaces in S^+ do not actually end up corresponding to connected components that intersect \mathbf{R} . However, we can use the stationarity statement of Proposition 3.1, and consider the picture of the quantum half-plane lying in front of η after a rational quantum time q , and note that for each quantum surface S_{t_i} in S^+ , there almost surely exists a rational time $q < t_i$ such the corresponding connected component has part of $\eta[0, \tau_q]$ on its boundary. We can then invoke our previous observation to see that the law of this quantum surface conditionally on its boundary length is also a quantum disk. We can therefore conclude that just as S^- , the Poisson point process S^+ is a Poisson point process of quantum disks.

Each excursion of η'' away from η' corresponds to exactly one CLE loop that is partially traced by η'' . As explained in [39], in order to complete this loop, one has to “branch inside” into the pocket disconnected by this excursion of η'' and η' , and trace an $\text{SLE}_\kappa(-\kappa/2)$ process there. This corresponds to tracing an $\text{SLE}_\kappa(-\kappa/2)$ in the bead of a quantum wedge of weight $3\kappa/2 - 4$. Part (ii) of Lemma 3.3 then allows one to conclude that the inside of the traced CLE loop is a quantum disk. Hence, this “first outside layer of loops” (the ones whose outer boundaries are part of η'') is formed of quantum disks. To conclude that this is the case of the inside of all CLE loops traced by η , one can just use the very same argument as above (combining the stationarity statement after any given rational time with this fact).

This concludes the fact that for the totally asymmetric $\text{SLE}_\kappa(\kappa - 6)$, the three Poisson point processes of quantum surfaces S^- , S^+ and S^ℓ are made of quantum disks, which in turn completes the proofs of Theorems 1.4 and 1.5 on the CLE exploration of quantum half-planes.

Remark 3.5. *It is worth noticing, that using similar arguments as in [18], one can show that it is possible to actually recover the whole initial quantum half-plane from the three Poisson point processes of discovered quantum disks. The analogous feature holds true also for the exploration of quantum disks and for the other explorations discussed in the next section.*

4. CLE EXPLORATIONS OF QUANTUM DISKS

We are now going to derive the form of the jump law for the boundary length evolution of a totally asymmetric $\text{SLE}_\kappa(\kappa - 6)$ process on an independent quantum disk. We will first study the chordal case (i.e., the exploration process starts from one boundary-typical point and is targeted at another)

by combining our results in the quantum half-plane with an absolute continuity argument. We will then deduce from this the results for other explorations.

The ideas in this section will be actually quite similar to those of [21] in the special case $\kappa = 6$.

4.1. The Radon-Nikodym derivative in the chordal case. Suppose now that $\mathcal{D} = (\mathbf{D}, h, -i, i)$ is a doubly marked quantum disk such that the quantum boundary length along the clockwise (resp. counterclockwise) segment of $\partial\mathbf{D}$ from $-i$ to i is equal to L_0 (resp. R_0). Let η be an independent $\text{SLE}_\kappa(\kappa - 6)$ in \mathbf{D} from $-i$ to i . We consider as before, the parameterization of its trunk by its natural quantum length. For each t , we denote by E_t the event that the trunk has not yet reached i at the (natural quantum) time t . On E_t , we define the quantum length of the left and right boundaries (L_t, R_t) of the remaining-to-be-discovered domain \mathcal{D}_t (at the time τ_t at which the trunk has natural length t). The process $\Delta_t = L_t + R_t$ corresponds to the quantum boundary length of \mathcal{D}_t , and this process will hit 0 when t reaches the total length of the trunk.

The key proposition of this section is the following:

Proposition 4.1. *On the event E_t , the Radon-Nikodym derivative between $(L_s, R_s)_{s \leq t}$ and the corresponding stable Lévy processes started from (L_0, R_0) as described in the setting of an $\text{SLE}_\kappa(\kappa - 6)$ exploration of a quantum half-plane is $\Delta_0^{\alpha+1} / \Delta_t^{\alpha+1}$. Furthermore, the domain \mathcal{D}_t is (when conditioned on its boundary length) a quantum disk.*

Proof. Let us consider a quantum half-plane in some domain D with marked boundary points that we call 0 and at ∞ . Let x_r (resp. x_l) be the point on the boundary which is r_0 (resp. l_0) units of quantum boundary length to the right (resp. left) of the origin. Recall that the domain with marked points x_r and ∞ is also a quantum half-plane.

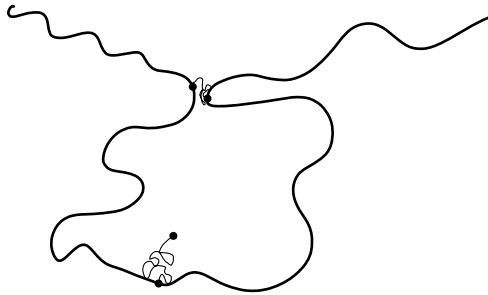


FIGURE 9. Symbolic sketch: The two pieces of η and η_r starting from 0 and x_r respectively, and the event F .

We let η and η_r be two $\text{SLE}_\kappa(\kappa - 6)$ processes starting from 0 and x_r respectively, both targeting ∞ and that are coupled so that they are part of the same $\text{SLE}_\kappa(\kappa - 6)$ exploration tree.

We are going to prove the proposition by considering an event F where η_r almost immediately cuts off a quantum disk of length close to $l_0 + r_0$ with 0 on its boundary. Conditionally on this event, η will locally evolve like an $\text{SLE}_\kappa(\kappa - 6)$ drawn in this quantum disk. On the other hand, one can also first let η evolve for a while (and we know what LQG surfaces it cuts out, since it is an $\text{SLE}_\kappa(\kappa - 6)$ on a quantum half-plane), and then look at how likely it is that F occurs. The sketch in Figure 9 is done in such a way to indicate that the event F in fact very much depends on the quantum half-plane (and less on the behavior of η_r).

More specifically, we fix $\epsilon > 0$ and let σ_ϵ be the first time that the left boundary length process associated with η_r makes a downward jump of size at least ϵ . Fix $\zeta \in (0, 1/2)$. We then let F_ϵ be the event that the quantum boundary length of the arc joining $\eta_r(\sigma_\epsilon)$ and 0 is contained in the interval $[l_0, l_0 + \epsilon^\zeta]$.

Let us now evaluate the probability of F_ϵ when $\epsilon \rightarrow 0$: We note that the supremum of the absolute value of the left boundary length process of η_r up to time σ_ϵ^- is very unlikely to be larger than $\epsilon^{2\zeta}$ when $\epsilon \rightarrow 0$, provided $\zeta > 0$ is chosen sufficiently small. We can for instance choose ζ so that this probability is bounded by $C\epsilon^3$. Noting that the jump from time σ_ϵ^- to σ_ϵ is taken from the intensity measure for the left boundary length process conditioned on the jump having size at least ϵ , which has density $c\epsilon^\alpha u^{-\alpha-1} \mathbf{1}_{[\epsilon, \infty)}(u)$, $c > 0$ a constant, with respect to Lebesgue measure, we see that

$$-C\epsilon^3 + \int_{l_0+r_0+\epsilon^{2\zeta}}^{l_0+r_0-\epsilon^{2\zeta}+\epsilon^\zeta} c\epsilon^\alpha u^{-\alpha-1} du \leq \mathbf{P}[F_\epsilon] \leq C\epsilon^3 + \int_{l_0+r_0-\epsilon^{2\zeta}}^{l_0+r_0+\epsilon^{2\zeta}+\epsilon^\zeta} c\epsilon^\alpha u^{-\alpha-1} du,$$

so that

$$(4.1) \quad \mathbf{P}[F_\epsilon] = c(1 + o(1))\epsilon^{\alpha+\zeta}(r_0 + l_0)^{-\alpha-1}.$$

Let \mathcal{F}_t be the filtration generated by the quantum surfaces cut off by η up to the moment when its trunk has reached quantum time t . Recall that the unbounded (i.e., with ∞ on its boundary) connected component of the complement of $\eta[0, \tau_t]$ with marked points η_{τ_t} and ∞ is a quantum half-plane \mathcal{W}_t .

When x_r and x_l have not yet been swallowed at this time (we call this event S_t , we can define \tilde{L}_t (resp. \tilde{R}_t) as the boundary length (in \mathcal{W}_t) between x_r and η_{τ_t} , and between x_l and η_{τ_t} respectively. Identity (4.1) applied to the evolution of η_r in \mathcal{W}_t shows that

$$\mathbf{P}[F_\epsilon | \mathcal{F}_t, S_t] = c(1 + o(1))\epsilon^{\alpha+\zeta}(\tilde{L}_t + \tilde{R}_t)^{-\alpha-1}.$$

Note also that the domain cut out by η_r at this time is then also a quantum disk of boundary length close to $\tilde{L}_t + \tilde{R}_t$ (in the $\epsilon \rightarrow 0$ limit, this will then ensure that the law of \mathcal{D}_t in the proposition is a quantum disk).

Hence, if A is an \mathcal{F}_t -measurable event with $\mathbf{P}[A, S_t] > 0$ and $\mathbf{P}[A, S_t | F_\epsilon] > 0$ then, as $\epsilon \rightarrow 0$,

$$\frac{\mathbf{P}[A, S_t | F_\epsilon]}{\mathbf{P}[A, S_t]} = \frac{\mathbf{P}[A, S_t, F_\epsilon]}{\mathbf{P}[F_\epsilon]\mathbf{P}[A, S_t]} = \frac{\mathbf{P}[F_\epsilon | A, S_t]}{\mathbf{P}[F_\epsilon]} = (1 + o(1)) \times \frac{(\tilde{L}_0 + \tilde{R}_0)^{\alpha+1}}{(\tilde{L}_t + \tilde{R}_t)^{\alpha+1}},$$

from which the proposition easily follows (one can for instance use scaling to compare the evolution in a disk of fixed boundary length Δ_0 with the evolution in a disk a boundary length close to Δ_0). \square

4.2. From the chordal to other CLE exploration mechanisms. Let us now briefly describe how to deduce Theorems 1.1 and 1.2 from Proposition 4.1. For this, we will study other $\text{SLE}_\kappa(\kappa - 6)$ exploration mechanisms (i.e., we will stick to the totally asymmetric $\text{SLE}_\kappa(\kappa - 6)$ but use different rules to decide in which direction to branch when it separates two domains).

- Before discussing further exploration mechanisms, let us first describe the laws of the jumps of the process (L, R) in the chordal exploration mechanism. Recall that for the half-plane process, the negative jumps of size ℓ by the boundary length correspond to swallowing a region by the trunk either to the left or to the right and both of these possibilities occur

at rate $a_-/\ell^{\alpha+1}$. We thus see that when one the rates of negative jumps from (L, R) to $(L - \ell, R)$ in the chordal exploration of a disk (with obvious notation) are

$$\frac{a_- \Delta^{\alpha+1}}{\ell^{\alpha+1} (\Delta - \ell)^{\alpha+1}} \times \mathbf{1}_{\ell < L}$$

and the corresponding formula for the jumps from (L, R) to $(L, R - \ell)$. So, the rate of negative jumps for $\Delta = L + R$ from Δ to $\Delta - \ell$, when the two boundary lengths are L and R is

$$\frac{a_- \Delta^{\alpha+1}}{\ell^{\alpha+1} (\Delta - \ell)^{\alpha+1}} \times (\mathbf{1}_{\ell < L} + \mathbf{1}_{\ell < R}).$$

Similarly, the positive jumps of the total boundary length process $\Delta = L + R$ can be described as follows: When $\Delta_t = \Delta$, it will jump to $\Delta + \ell$ with a rate proportional to $(a_+/\ell^{\alpha+1}) \times (\Delta^{\alpha+1}/(\ell + \Delta)^{\alpha+1})$. Mind that they depend on (L, R) only via Δ .

- A natural variant of the chordal exploration of the quantum disk is, at each splitting time at which a quantum surface is actually cut off by the trunk (so the domain with quantum boundary length Δ splits into two domains of boundary length ℓ and $\Delta - \ell$), to choose to branch into the domain with largest boundary length. In other words, one chooses to go into the domain with boundary length ℓ if and only if $\ell > \Delta/2$. We will refer to this as the $(q = \infty)$ -exploration mechanism.

One way to approximate this process is, at each time at which the quantum natural time of the trunk is a multiple $n\epsilon$ of ϵ , to change the target point of the chordal exploration, and to choose it to be the “antipodal” point of the exploration point (so that at this time, the boundary lengths of the two boundary arcs from that point to the target point are identical and equal to $\Delta_{n\epsilon}/2$). Then, during the time-interval $[n\epsilon, (n+1)\epsilon]$ one uses the chordal exploration with this target point. When ϵ tends to 0, this approximation converges to this exploration variant (indeed, it is going to be the same on any bounded time-interval, provided ϵ is small enough).

Our previous description of the boundary length process in the chordal case can be transcribed in terms of the jumps of the chordal exploration for this variant. First, the positive jumps of all the total boundary length process will remain the same as for the chordal exploration, as it is not affected by the branching rule (i.e., the process does not branch at those times). For the negative jumps, one gets a rate

$$\frac{2a_- \Delta^{\alpha+1}}{\ell^{\alpha+1} (\Delta - \ell)^{\alpha+1}} \times \mathbf{1}_{\ell < \Delta/2}$$

and the Lévy compensation is just as in the exploration of the quantum half-plane.

This completes the proofs of Theorem 1.1 and 1.2, up to proving Lemma 3.3 which will be completed in the appendix.

Note also that the side-swapping approximation of $\text{SLE}_\kappa^\beta(\kappa - 6)$ processes immediately implies the analogous statement for those processes (with appropriate branching mechanism) when drawn on a quantum disk.

It is worth mentioning here that other exploration mechanisms (i.e., rules on how to branch when the domain is split into two smaller ones) of quantum disks are quite natural to consider. In particular, one can choose a fixed $q > \alpha$, and, at each splitting time – when the two “available” domains have respective boundary lengths ℓ and $\Delta - \ell$, to choose to branch into them with respective probabilities $\ell^q/(\ell^q + (\Delta - \ell)^q)$ and $(\Delta - \ell)^q/(\ell^q + (\Delta - \ell)^q)$. The choice of q ensures that during each positive

time interval, the probability that this variant does actually coincide with the exploration that always chooses the domain with largest available boundary length is positive, so that it is possible to define this q -exploration mechanism as a simple modification of the one that branches into the largest one (which corresponds to $q = \infty$). The case where $q = \alpha + 1/2$ will actually turn out to be natural in view of the next section.

4.3. BCLE on LQG discussion. Let us rephrase some of the previous results in terms of the boundary conformal loop ensembles introduced in [39] (we refer to this paper for a definition of these natural ensembles of loops). Let us now consider the trunk η' of the totally asymmetric $\text{SLE}_\kappa(\kappa - 6)$ drawn on an independent quantum disk (but starting from a boundary typical point and targeting another boundary typical point). On the one hand, we know that the connected components of the complement of η' that are totally surrounded by η' are all quantum disks conditionally on their boundary lengths. If we then consider one of these connected components \mathcal{D} that is surrounded clockwise, then the loop-trunk decomposition of η indicates that in order to trace the rest of η in this connected component, one has to trace a $\text{BCLE}_\kappa(3\kappa/2 - 2)$ (or equivalently a $\text{BCLE}_\kappa(-\kappa/2)$ if one orients it in the other way). But we have just shown that the connected components traced by this BCLE will consist of independent quantum disks given their boundary length. In other words, when one traces an independent $\text{BCLE}_\kappa(3\kappa/2 - 2)$ on top of an independent quantum disk, then all the connected components will be quantum disks conditionally on their boundary lengths.

In fact, if we apply the very same argument to the side-swapping $\text{SLE}_\kappa^\beta(\kappa - 6)$, we get the following general statement that is interesting on its own right:

Proposition 4.2 (BCLE on quantum disks). *Suppose that $\kappa \in (8/3, 4)$ and that ρ is in the admissible interval $(\kappa/2 - 4, \kappa/2 - 2)$ so that one can define a $\text{BCLE}_\kappa(\rho)$. Conditionally on their boundary lengths, the connected components of the complement of a $\text{BCLE}_\kappa(\rho)$ traced on an independent quantum disk are all quantum disks.*

This result actually also holds for $\kappa \in (2, 8/3]$, and can be derived more directly, but the proof used here (for presentation purposes) only works for $\kappa \in (8/3, 4)$. Actually, see [38], the statement is also valid for the BCLEs with κ' instead of κ .

5. THE NATURAL QUANTUM MEASURE IN THE CLE CARPET

5.1. Preamble. Theorems 1.1 and 1.2 show that it is possible to transcribe questions about CLE on LQG disks in terms of features of some explicit multiplicative cascade-type processes that are built on variants of asymmetric Lévy processes. These multiplicative cascades have actually been studied in their own right (they are also closely related to branching random walks) and a number of results that are actually available in the literature can be rather directly applied to construct natural objects related to CLE on LQG surfaces. This is illustrated in this section with the natural LQG measure that lives in the CLE carpet – this is a natural object to consider in view of the scaling limit of decorated planar maps or of planar maps with large faces [6, 5, 13, 15] (as the suitably renormalized number of points in the latter should converge to the natural LQG measure on the CLE carpet).

We would like to emphasize one point here: As shown in [40], when one explores a CLE using an $\text{SLE}_\kappa(\kappa - 6)$ curve for $\kappa \in (8/3, 4)$, one uses some extra randomness that is not present in the CLE_κ (i.e., the $\text{SLE}_\kappa(\kappa - 6)$ process is not a deterministic function of the CLE_κ). In other words, in the exploration tree of CLE on LQG that gives rise to the branching trees and to the

multiplicative cascades, one uses three random inputs: (i) The randomness used to define the CLE, (ii) the randomness of the LQG and (iii) the additional randomness of the CPI curve used to draw the trunk of the $\text{SLE}_\kappa(\kappa - 6)$. So, when one constructs some random variables using the branching tree, some additional work is needed to check (if it is the case) that they are in fact a deterministic function of (i) and (ii) only. In the present case, the measure is the one that appears in the papers [5, 15] and the contribution of this section is to show that it is indeed a function of the CLE and LQG measure only.

This section will be structured as follows. For the readers who are not so acquainted with the results on these multiplicative cascades and as a warm-up to Section 5.3, we briefly survey in Section 5.2 some of the basic general features that we will use here. We recall some results of [5] who construct the “natural area measure” on the boundary of the branching tree \mathcal{T} . Finally, in Section 5.3, building also on a result of [15], we show Theorem 1.3 which proves that this measure is indeed a function of the CLE and the LQG measure only.

5.2. Background and heuristics: Construction of the measure. Suppose that we are given a law \mathcal{U} on random decreasing families of positive reals $U := (U_n)_{n \geq 0}$ such that $\mathbf{E}[\sum_{n \geq 0} U_n] = 1$. This is viewed as the law of the collection of smaller fragments that an object of size 1 gets fragmented into (an object of size x would be fragmented into a collection with sizes distributed like $(xU_n)_{n \geq 0}$). We suppose that we are given an i.i.d. copies of U that we denote by U^{n_1, \dots, n_j} that are indexed by finite sequences of non-negative integers. The multiplicative cascade $(M_j)_{j \geq 0}$ is then defined by $M_0 = 1$ and

$$M_j := \sum_{n_1, \dots, n_j} U_{n_1} U_{n_2}^{n_1} \dots U_{n_j}^{n_1, \dots, n_{j-1}}.$$

These cascades are clearly positive martingales. It is known that they converge in L^1 to a positive limit M_∞ as soon as there exists $r > 1$ such that $\mathbf{E}[\sum_n (U_n)^r]$ and $\mathbf{E}[(\sum_n U_n)^r]$ are both finite (these types of results were first established in the setting of branching random walks, see [8, 9, 31]). When such a convergence in L^1 holds, it is possible to also obtain convergence along “stopping lines” in the branching tree (using generalizations of the optional stopping theorem, so that the value of M on this stopping line is the conditional expectation of M_∞ given the information discovered before that line, see e.g., [9]).

Such multiplicative cascades arise naturally in the settings of the tree structures \mathcal{T} and $\tilde{\mathcal{T}}$. Let us quickly explain how to quickly identify such a martingale in the latter case, using the fact that the expected value of the quantum area \mathcal{A} of a quantum disk of boundary length 1 is finite (we will briefly recall how to derive this fact in Remark 5.4). One can draw on this quantum disk an independent nested CLE_κ . Exploring such a nested CLE_κ provides (when the CPI branches are parameterized by the quantum length) exactly the branching structure \mathcal{T} (this follows from our previous results, since in each of the discovered CLE_κ loops, the process continues its exploration). If one explores the nested CLE_κ up to some “finite depth” (meaning for instance L that one has not explored inside any of the k th level CLE_κ loops for some finite k), then simply because the CLE_κ carpets have zero Lebesgue measure, it follows that \mathcal{A} is equal to the sum of the areas of the remaining-to-be-explored disks. If we order their boundary lengths in decreasing order by L_0, L_1, \dots , we immediately get (using the scaling rule for the area) that $\mathcal{A} = \sum_{n \geq 0} L_n^2 \mathcal{A}_n$, where $(\mathcal{A}_n)_{n \geq 0}$ is a collection of i.i.d. copies of \mathcal{A} . In particular, if \mathcal{F} denotes the information collected before this partial exploration, one gets $\mathbf{E}[\mathcal{A} | \mathcal{F}]$ is equal to $\sum_{n \geq 0} L_n^2$. So, we see readily that when one chooses $(U_n)_{n \geq 0}$ to have the law of $(L_n^2)_{n \geq 0}$, then one is in the previous setting. The fact that $M_1 = \mathbf{E}[\mathcal{A} | \mathcal{F}]$ readily implies that the martingale is uniformly integrable and converges in L^1 and almost surely to

\mathcal{A} (so in this particular case, the convergence result can be derived directly, without referring to the general results on these cascades).

Let us now turn our attention to the tree \mathcal{T} . Suppose that we are using the aforementioned ($q = \infty$)-exploration (corresponding to the CLE exploration of an LQG disk that always branches into the largest of the two available choices). We choose to stop exploring this branch at the first time at which the boundary length of the currently “to-be-explored” disk exits the interval $[1/2, 2]$ (this choice turns out to be convenient for our purposes here). At that time T , we order the to-be-explored disks in the carpet in decreasing order l_0, l_1, \dots . Note that all the l_n ’s with the only possible exception of l_0 are smaller than 1.

We can also interpret the same exploration as an exploration of the larger tree-structure $\tilde{\mathcal{T}}$. In other words, we keep track of the positive jumps corresponding to the discovered CLE loops as well as the l_n ’s. In this setting, at time T , one then has a larger collection of to-be-explored disks with boundary lengths L_0, L_1, \dots , where (l_n) forms a subsequence of (L_n) . Note that by construction, all of the L_n ’s are smaller than 1, with the possible exception of L_0 and L_1 . The same argument as above shows that $\mathbf{E}[\sum_{n \geq 0} L_n^2] = 1$.

It is easy to get some crude information on the joint law of $(l_n)_{n \geq 0}$:

- (1) The law of T has an exponential tail (just because of the lower bound on positive jumps of size greater than 2 before T).
- (2) The largest boundary length l_0 has a polynomial tail distribution of the type $cx^{-2\alpha-1} \leq \mathbf{P}[l_0 \geq x] \leq Cx^{-2\alpha-1}$ as $x \rightarrow \infty$ (this just comes from the fact that the intensity measure of positive jumps is bounded from above and from below by a constant times $dl/l^{2\alpha+2}$ as $l \rightarrow \infty$) for some absolute constants c and C .
- (3) One has also good information about the numbers of small positive and small negative jumps before T . For instance, by trivially bounding the intensity rates of negative jumps of size l before time T by a constant times $1/l^{\alpha+1}$, one sees readily that conditionally on T , the expected number of l_n ’s that lie in $[2^{-k}, 2^{-k+1}]$ is bounded by $C2^{\alpha k}T$ for some constant C .

Such estimates can then be easily combined to check that $\mathbf{E}[\sum_n l_n^\beta] < \infty$ for all $\beta \in (\alpha, 2\alpha + 1)$. Furthermore, this quantity will tend to ∞ as $\beta \rightarrow \alpha$ (using the lower bound on the tail of l_0), and we know on the other hand that $\mathbf{E}[\sum_n l_n^2] < \mathbf{E}[\sum_n L_n^2] = 1$. It follows that there exists a value $\delta \in (\alpha, 2)$ such that $\mathbf{E}[\sum_n l_n^\delta] = 1$. We will see in a moment that δ is in fact equal to $\alpha + 1/2$ but this will not be needed at this point. So, if we choose $(U_n := l_n^\delta)_{n \geq 1}$, then we are in the setup described above. One can check (using the previous type of estimates on the joint law of l_n ’s) that the L^1 -convergence criteria are fulfilled. In particular, one can then deduce that if M_∞ denotes the limit of the martingale M_n , and if one stops the exploration of the tree at any “finite” stopping line, the sum of the δ -th powers of the boundary length of the remaining-to-be-explored disks is equal to the conditional expectation of M_∞ . All this corresponds exactly to the convergence of the *Malthusian* martingales in the branching structure \mathcal{T} stated in [5], see also [15, Section 3.1].

The random variable $Y := M_\infty$ is then interpreted as the “total natural quantum mass” of the CLE carpet. It is actually possible to use the same ideas in order to define an LQG measure on the CLE carpet: When O is some given open set, we can define the stopping line S in the exploration tree, when one stops exploring at each time the remaining to be explored disk is entirely contained in O . Mind that for a substantial portion of the branching tree, S would be infinite (it corresponds to points that are not in O). In that way, one gets a collection D_1, D_2, \dots of to-be-explored disks at time S . Then, the previous construction allows one to make sense of the mass of each of the carpets

of these disks, and we *define* $\mathcal{Y}(O)$ to be the sum of all these masses. One can then show that \mathcal{Y} corresponds to a proper measure in the CLE carpet, with total mass M_∞ . We will see in the next section another way to construct \mathcal{Y} as a limit of some simple measures.

Let us stress again that this construction of Y (and of \mathcal{Y}) uses the randomness that is given by the exploration tree, so that it is not clear at this stage whether it is a deterministic function of the LQG measure and the CLE.

Remark 5.1. *Following the ideas of [32] (this is also mentioned and used in [15]), it is possible to describe the time-reversal of the exploration process that is targeting a point chosen according to the quantum natural measure \mathcal{Y} on the carpet, in terms of another Lévy process. This type of feature can be useful in the context of planar maps, as it would correspond to exploring the map towards a uniformly chosen point. Note also that further features, such as the conditional law of \mathcal{T} given Y , or properties of the law of Y are derived in the recent paper [7].*

Remark 5.2. *The quantity Y is called the intrinsic area of the growth-fragmentation tree \mathcal{T} in [5, 7]. This terminology comes from the fact that this tree arises as scaling limit of peeling processes on random planar maps with large faces, and that this intrinsic area then corresponds to the scaling limit of the counting measure on these planar maps. But this does not quite show that in our setup, \mathcal{Y} does depend on the CLE and the LQG measure only.*

Remark 5.3 (Comment on the value of the exponent). *The fact that $\delta = \alpha + 1/2$ is actually stated in [5, Proposition 5.2]. Indeed, the particular, the jump measure described in the displayed equation just before (28) in [5] is precisely the one that we are investigating here, so that we are looking for the value of $q \in (\alpha, 2)$ for which $\kappa_\alpha(q) = 0$ in the last formula of [5, Proposition 5.2], which is obviously $q = \alpha + 1/2$ (due to the $\cos(\pi(q - \alpha))$ term).*

Note that [5, Proposition 5.2] and its proof give a more general result than the particular case that we need here. Proving that $\delta = \alpha + 1/2$ directly is actually not easy to perform without the help of a software package like Mathematica for guidance about the right change of variables. One has to check that the contribution of the positive jumps, of the negative jumps and of the Lévy compensation for this process exactly cancel out. In particular, one has to evaluate the asymptotics as $\epsilon \rightarrow 0$

$$\int_\epsilon^\infty \frac{-\cos(4\pi/\kappa)dl}{l^{\alpha+1}(1+l)^{\alpha+1}}((1+l)^{\alpha+1/2} - 1) - \int_\epsilon^{1/2} \frac{dl}{l^{\alpha+1}(1-l)^{\alpha+1}}(l^{\alpha+1/2} + (1-l)^{\alpha+1/2} - 1).$$

Actually, an indication of the fact that $\delta = \alpha + 1/2$ (that could be turned into a lengthy and very convoluted proof compared to the previous direct computation) is to notice that the Hausdorff dimension of the CLE_κ carpet (in the Euclidean metric) for $\kappa \in (8/3, 4]$ is known to be almost surely equal to $D = 2 - (8 - \kappa)(3\kappa - 8)/(32\kappa)$ (see [45] for the upper bound and the result for the “expectation dimension” which is the relevant one to apply the KPZ ideas – see [41] for the lower bound). On the other hand, this CLE carpet is independent of the LQG measure, so that the KPZ ideas from [19] should be applicable here. And, when one applies the KPZ formula, one indeed gets the formula $\delta = \alpha + 1/2$.

Remark 5.4 (Finite expectation). *For sake of completeness, let us provide one quick proof of the fact (that will also be used in the next section) that the expected quantum area of a disk of boundary length 1 is finite i.e., that $\mathbf{E}[\mathcal{A}] < \infty$ in the notation used above. In fact, the slightly stronger fact holds:*

Lemma 5.5. *One has $\mathbf{E}[\mathcal{A}^p] < \infty$ for all $p \in (0, 4/\gamma^2)$.*

Proof. Let \mathcal{M} be the infinite measure on quantum disks and suppose that $(\mathcal{S}, h, -\infty, +\infty)$ is defined under this infinite measure \mathcal{M} . Let E be the set of h such that the boundary length ℓ is in $[1, 2]$. This set has finite and positive mass for \mathcal{M} , so that we can define the probability measure $\mathcal{M}_{[1,2]}$ to be \mathcal{M} restricted to this set and properly renormalized. Keeping the scaling rule in mind, we therefore immediately see that the law of the quantum area \mathcal{A} of a quantum disk with boundary length 1 is dominated by that of a quantum disk defined under the law $\mathcal{M}_{[1,2]}$. So, it is sufficient to show that for $p \in (0, 4/\gamma^2)$ close to $4/\gamma^2$,

$$\mathcal{M}[\mathbf{1}_{\ell \in [1,2]} \mathcal{A}^p] < \infty.$$

For each $u \in \mathbf{R}$, we let X_u be the average of h on the vertical segment $u + (0, i\pi)$ and define $X^* := \sup_{u \in \mathbf{R}} X_u$. Recall that conditionally on X^* , X looking forward and looking backward after this maximum are independent Brownian motions run at twice the speed with negative drift $\gamma - Q = \gamma/2 - 2/\gamma$ and conditioned not to exceed X^* . Then the measure under which X^* is defined is a multiple of $e^{-\lambda x} dx$ with $\lambda = 2/\gamma - \gamma/2$.

We will decompose \mathcal{M} according to the value of X^* as this turns out to be a handy description of \mathcal{M} to make computations and estimates. In the sequel, \mathcal{M}_x will denote the probability measure where $X^* = x$, so that $\mathcal{M} = \int_{\mathbf{R}} C e^{-\lambda x} \mathcal{M}_x dx$.

Let us first study the part of the integral when X^* is negative. It is easy to check (using the scaling rule for the quantum area) that

$$\mathcal{M}[\mathbf{1}_{\ell \in [1,2]} \mathcal{A}^p \mathbf{1}_{X^* < 0}] \leq \mathcal{M}[\mathcal{A}^p \mathbf{1}_{X^* < 0}] = \mathcal{M}_0[\mathcal{A}^p] \int_{-\infty}^0 C e^{-\lambda x} e^{p\gamma x} dx$$

for some finite constant C . By [42, Proposition 3.5], we know that $\mathcal{M}_0[\mathcal{A}^p] < \infty$ for $p \in (0, 4/\gamma^2)$. Moreover, the integral is finite as soon as $p > \lambda/\gamma$. Note that $\lambda/\gamma = 2/\gamma^2 - (1/2) < 4/\gamma^2$, so this includes the cases where p is close to $4/\gamma^2$.

For the positive values of X^* , if u^* denotes the value such that $X^* = X_{u^*}$, then we define ℓ' to be the boundary length of the segment joining $(u^*, u^* + 1)$ (we again view \mathcal{S} as a subset of the complex plane). Then, for any positive r , using Markov's inequality and the scaling-rule, we have

$$\mathcal{M}_x[\mathbf{1}_{\ell \in [1,2]}] \leq \mathcal{M}_x[\mathbf{1}_{\ell' \leq 2}] \leq \mathcal{M}_x[\mathbf{1}_{(2/\ell')^r \geq 1}] \leq \mathcal{M}_x[(2/\ell')^r] = e^{-\gamma r x/2} \mathcal{M}_0[(2/\ell')^r].$$

But [42, Proposition 3.6], we know that this last expectation is finite for any $r > 0$. On the other hand, scaling shows that

$$\mathcal{M}_x[\mathcal{A}^{p''}] = e^{p'' \gamma x} \mathcal{M}_0[\mathcal{A}^{p''}],$$

and [42, Proposition 3.5] gives that this last expectation is finite as soon as $p'' < 4/\gamma^2$.

We can now wrap up: When $p < 4/\gamma^2$, we now choose $p' > 1$ so that $p'' := pp' < 4/\gamma^2$, and we let $q' > 1$ be such that $(1/p') + (1/q') = 1$. By Hölder's inequality,

$$\mathcal{M}[\mathbf{1}_{\ell \in [1,2]} \mathcal{A}^p \mathbf{1}_{X^* > 0}] = \int_0^\infty C e^{-\lambda x} \mathcal{M}_x[\mathcal{A}^p \mathbf{1}_{\ell \in [1,2]}] dx \leq \int_0^\infty C \mathcal{M}_x[\mathcal{A}^{pp'}]^{1/p'} \mathcal{M}_x[\mathbf{1}_{\ell \in [1,2]}]^{1/q'} dx$$

This integral is finite as the first term is equal to a constant times $e^{\gamma p x}$ while the second one decays faster than $\exp(-rx/q')$ (for any given r , so in particular for $r = 2q'\gamma p$) as $x \rightarrow \infty$. \square

5.3. Uniqueness of the LQG carpet measure. Our goal in this section is to show that the random variable Y that is described in the previous section is equal to the limit in probability of some constant times $\epsilon^{\alpha+1/2}$ times the number $N_{[\epsilon, 2\epsilon]}$ of outermost CLE loops with quantum boundary lengths in $[\epsilon, 2\epsilon]$. As such a description of Y only depends on the CLE and on the LQG measure, proving this statement would indeed show that Y is independent of the additional randomness that comes from the exploration tree (and it concludes the proof of Theorem 1.3).

Let us first emphasize that this can again be viewed a statement about the labeled branching tree \mathcal{T} only. Indeed $N_{[\epsilon, 2\epsilon]}$ is just the total number of “positive jumps” of size in $[\epsilon, 2\epsilon]$ in the tree. So, in a way, one needs to transfer the previous construction of Y (that was given more in terms of number of small negative jumps) into a description in terms of small positive jumps. While certainly not surprising to any specialist of these trees, this statement does not seem to be written up in the existing literature, so we provide a proof here. Before that, let us provide a brief heuristic description of what is going on.

The random variable Y describes the number of small LQG disks in which the CLE exploration divides the CLE carpet into (let us stress again that we are dealing with \mathcal{T} here, and do not care about the domains encircled by CLE-loops). It is for instance actually shown in [15, Theorem 3.4] that if we stop the exploration mechanism in each branch of the tree \mathcal{T} as soon as the label becomes smaller than ϵ (we will refer to this as the “stopping line” \mathcal{L}_ϵ for this tree), then the empirical measure μ_ϵ of the sizes of the collection of obtained labels behaves like $\epsilon^{-\alpha-1/2} \times Y \times \nu(\epsilon \cdot)$ as $\epsilon \rightarrow 0$, where ν is some finite measure on $[0, 1]$. In particular, $\epsilon^{\alpha+1/2}$ times the number of disks-sizes/labels between $\epsilon/2$ and ϵ in this “stopping line” will converge in L^1 to some constant times Y . This suggests that the number of CLE loops with boundary length of the order of ϵ should also explode like some constant times $Y\epsilon^{-\alpha-1/2}$. Indeed, a typical small CLE loop will be discovered by the exploration within a disk of boundary length of the same order of magnitude as the boundary length of the CLE loop.

There are a number of possible concrete ways to turn the previous heuristics into a proof, building on the available results in the literature. Here is one outline, that builds on the aforementioned fact:

Proposition F (Special case of Theorem 3.4 in [15]). *Let us denote the boundary lengths appearing at the stopping line \mathcal{L}_y in decreasing order by Y_1^y, Y_2^y, \dots . There exists a deterministic measure ν on $[0, 1]$, such that when F is a measurable non-negative function on $[0, 1]$,*

$$y^{\alpha+1/2} \sum_{n \geq 1} F(Y_n^y/y) \rightarrow Y \times \int F(u) d\nu(u)$$

in L^1 as $y \rightarrow 0$.

Then:

- (1) Let us first make some simple a priori estimates. Note that the expectation of the number $N_{[x, \infty]}$ of upwards jumps of size greater than x in the tree \mathcal{T} (when started from a quantum disk of boundary length equal to 1) is finite; it is actually trivially bounded by $1/x^2$ as the expected quantum area C of the initial disk (here we mean the quantum area of the entire disk) is bounded from below by $\mathbf{E}[N_{[x, \infty)} C x^2]$ (just sum the area of all the disks corresponding to the CLE_κ loops of boundary length greater than x).

Next we can note that as $x \rightarrow 0$, the quantity $N_{[x, 2x]} x^{\alpha+1/2}$ is bounded from below by some positive (random) number. We can for instance use the aforementioned result about

the number of disks of boundary length in $[\epsilon/2, \epsilon]$ on the stopping line \mathcal{L}_ϵ , and note that for each of these disks, the probability to then make a positive jump of size in $[x, 3x/2]$ (for any choice of $x \in [\epsilon/2, 2\epsilon]$) is bounded from below.

- (2) When $y \geq 4x$, let $N_{[x, 2x]}^y$ (resp. $D_{[x, 2x]}^y$) denote the total number of positive (resp. negative) jumps of size in $[x, 2x]$ that occur before the stopping line \mathcal{L}_y . By comparing the jump rates of positive and negative jumps (noting that the latter is always bounded by the former for a given small-enough jump-size),

$$\mathbf{E}[N_{[y/2, y]}^{2y}] \leq C\mathbf{E}[D_{[y/2, y]}^{2y}]$$

for some constant C . But by construction, we note that

$$\mathbf{E}[D_{[y/2, y]}^{2y}] \leq \mathbf{E}\left[\sum_{n \geq 1} \mathbf{1}_{Y_n^{2y} \in [y/2, y]}\right] \leq C'y^{-\alpha-1/2}$$

for some constant C' (this follows for instance from Proposition F). By comparing the jump rates of positive jumps of size in $[Mx, 2Mx]$ and of positive size in $[x, 2x]$ at times at which the labels are greater than $4Mx$, we then see that for some constant C'' that is independent of M and x ,

$$\mathbf{E}[N_{[x, 2x]}^{4Mx}] \leq M^\alpha \mathbf{E}[N_{[Mx, 2Mx]}^{4Mx}] \leq C''M^{-1/2}x^{-\alpha-1/2}.$$

In particular, using Markov's inequality, we see that for any given δ , if we choose M very large, we can ensure that

$$\mathbf{P}[N_{[x, 2x]}^{4Mx}x^{\alpha+1/2} \geq \delta] \leq \delta$$

for all small x .

- (3) We now fix a very large M and will study the parts of the tree *after* the stopping line \mathcal{L}_y for $y = 4Mx$ (we will use this value of y from now on). We denote by $Q_{[x, 2x]}^y = N_{[x, 2x]}^y - N_{[x, 2x]}^y$ the number of positive jumps of size in $[x, 2x]$ after that line. Recall that at this stopping line \mathcal{L}_y , one has a collection of disks of boundary lengths Y_1^y, Y_2^y, \dots . For each n , we denote by Z_n^y the number of (outermost) CLE loops with quantum boundary length in $[x, 2x]$ that respectively lie in the disk of boundary length Y_n^y , so that $Q_{[x, 2x]}^y = \sum_{n \geq 1} Z_n^y$. Our goal is to show that the quantity $x^{\alpha+1/2}Q_{[x, 2x]}^y$ converges in probability to some constant times Y . For each n , we let \bar{Z}_n^y denote the conditional expectation of Z_n^y given Y_n^y .

Let $F_0(z)$ denote the expected number of (outermost) CLE loops of quantum boundary length in $[z/(4M), 2z/(4M)]$ in a CLE drawn on a quantum disk of boundary length 1. We can first apply Proposition F to $F(z) = F_0(z)\mathbf{1}_{z \leq \epsilon/(4M)}$, and see that it implies that when ϵ is chosen to be very small,

$$x^{\alpha+1/2} \sum_{n \geq 1} \bar{Z}_n^y \mathbf{1}_{Y_n^y \leq \epsilon x}$$

converges in L^1 to some random variable that has a very small expectation. In particular, we deduce readily that for all given δ , when ϵ is chosen small enough,

$$\mathbf{P}\left[x^{\alpha+1/2} \sum_{n \geq 1} Z_n^y \mathbf{1}_{Y_n^y \leq \epsilon x} \geq \delta\right] \leq \delta$$

for all x .

(4) It remains to show that for fixed large M and a fixed small ϵ ,

$$x^{\alpha+1/2} \sum_{n \geq 1} Z_n^y \mathbf{1}_{Y_n^y > \epsilon x}$$

converges in probability to some constant times Y . Here, we can first apply the same argument as above to the function $F(z) = F_0(z) \mathbf{1}_{z \geq \epsilon/(4M)}$ to see that

$$x^{\alpha+1/2} \sum_{n \geq 1} \bar{Z}_n^y \mathbf{1}_{Y_n^y > \epsilon x}$$

converges in probability to a constant times Y . Hence, it remains to argue that

$$x^{\alpha+1/2} \sum_{n \geq 1} (Z_n^y - \bar{Z}_n^y) \mathbf{1}_{Y_n^y > \epsilon x}$$

converges to 0 in probability. This is now essentially a variation of the law of large numbers: When x is small and one conditions on the values Y_n^y, \dots , this is bounded by a constant times the mean of a large number m_x (that is greater than some positive number times $x^{-\alpha-1/2}$ with high probability) of independent random variables of mean 0, and one has good uniform integrability control on these variables because of the integrability of the quantum area \mathcal{A} of a quantum disk with boundary length 1 (i.e., Lemma 5.5). More specifically, let c denote the probability that a quantum disk with boundary length 1 has an quantum area at least 1, and let c' denote the infimum over all positive m that the sum of m independent Bernoulli random variables, that are each equal to 1 with probability c , is greater than $mc/2$. Then, by bounding the sum of the quantum areas of the Z_n^y to be explored disks by the area of the disk with boundary length Y_n^y , and using the scaling properties, we immediately see that for all k , and all n with $Y_n^y > \epsilon x$,

$$c' \mathbf{P}[Z_n^y > k] \leq \mathbf{P}[\mathcal{A} > (k/2) \times (\epsilon/2M)^2],$$

which is sufficient to conclude.

APPENDIX A. PROOF OF LEMMA 3.3

Let us start with the following general statement, that will be one key to the proof of Lemma 3.3.

Lemma A.1. *Fix $W \in (0, \gamma^2 - 2)$. Suppose that \mathcal{B} is a bead of a quantum wedge of weight W with left (resp. right) boundary length conditioned to be equal to 1 (resp. ϵ). Then in the limit as $\epsilon \rightarrow 0$, \mathcal{B} converges to a unit boundary length quantum disk.*

The sense of convergence that we consider in Lemma A.1 is the following. Let $z \in \mathcal{B}$ be chosen from the quantum measure and let h be the field obtained by embedding \mathcal{B} into \mathbf{D} using a conformal transformation which takes z to 0 and post-composed with a rotation by a uniformly random angle. Then for any finite collection ϕ_1, \dots, ϕ_n of $C_0^\infty(\mathbf{D})$ functions we have that the joint law of (h, ϕ_j) for $1 \leq j \leq n$ converges as $\epsilon \rightarrow 0$ to that when h is the field which describes a unit boundary length quantum disk with the same embedding (uniformly random interior point taken to the origin post-composed with a rotation with a uniformly random angle).

Throughout this appendix, we say that a bead of a wedge has boundary length (l, r) if the clockwise (resp. counterclockwise) boundary arcs of the wedge have respective lengths l and r .

Proof. Suppose that $\mathcal{D} = (\mathbf{D}, h, -i, i)$ is a quantum disk with boundary length 1. Let x be the point on the unit circle so that the counterclockwise arc connecting $-i$ and x has quantum length ϵ , so that $(\mathbf{D}, h, -i, x)$ is a bead of a $\gamma^2 - 2$ wedge with boundary lengths $(1 - \epsilon, \epsilon)$. Let η_x be an independent $\text{SLE}_\kappa(W - 2; \kappa - 4 - W)$ process in \mathcal{D} from $-i$ to x . We know from Theorem B-(ii) applied to the thin wedge of weight $\gamma^2 - 2$ (the beads of which are disks) that the quantum surfaces parameterized by the components of $\mathbf{D} \setminus \eta$ which are to the left of η are beads of a wedge of weight W – in particular, this will hold for the component \mathcal{B} with the largest boundary length.

The goal is now to study what happens if we let ϵ tend to 0. Conditionally on the boundary lengths (L, R) of its two sides, \mathcal{B} has the law of a bead of a wedge of weight W (with those boundary lengths). Moreover, we can note that (simply because η gets smaller and smaller in \mathbf{D} in this setup), \mathcal{B} converges to \mathcal{D} itself as $\epsilon \rightarrow 0$ i.e., it becomes a quantum disk with unit boundary length. So, we have the convergence of some bead of a quantum wedge of weight W to a quantum disk as in the Lemma. However, the boundary lengths (R, L) of this bead are here random (but when ϵ is small, then R is small and L is close to 1), so some little work is needed to deduce the lemma itself.

Let us first provide more information about the law of (L, R) . Let $\varphi: \mathbf{D} \rightarrow \mathbf{H}$ be the unique conformal map which sends $-i$ to 0, x to 1, and i to ∞ . We know from the definitions of a quantum disk and quantum half-plane that

$$h \circ \varphi^{-1} + Q \log |(\varphi^{-1})'| + \frac{2}{\gamma} \log \frac{1}{\epsilon}$$

converges as $\epsilon \rightarrow 0$ to the law of a quantum half-plane (embedded so that the boundary length of $[0, 1]$ is 1), in the strong sense of convergence is that the restriction of the field/path pair to any compact set converges in total variation). Let X be the quantum length of the part of the boundary of the unbounded component of $\mathbf{H} \setminus \varphi(\eta)$ which is on $\varphi(\eta)$ and let Y be the quantum length of the part of $\partial\mathbf{H}$ which is cut off from ∞ by η . It follows from the above convergence that the law of $\epsilon^{-1}(1 - L, R)$ converges in total variation to the law of (X, Y) as $\epsilon \rightarrow 0$. Hence, if we combine this with the conclusion of the previous paragraph we get that if we consider a bead of a wedge with weight W and respective boundary lengths $(1 - \epsilon X, \epsilon Y)$, then as $\epsilon \rightarrow 0$, it converges (in distribution) to a quantum disk with unit boundary length. By simple scaling, the same will hold true if we take the boundary lengths to be $(1, \epsilon Y / (1 - \epsilon X))$.

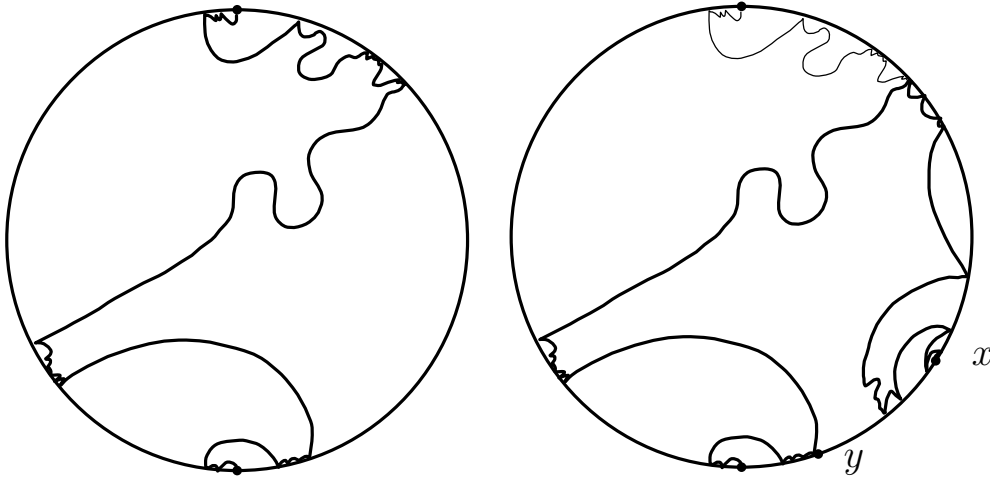
Finally, we can note that the convergence of \mathcal{B} to \mathcal{D} is in fact a convergence in probability, so that the conditional law of \mathcal{B} given (L, R) is close to its unconditioned law (from which one can see that it is possible to condition on the values of X and Y in the previous statement). \square

We are now ready to prove Lemma 3.3.

Proof of Lemma 3.3. We will focus on completing the proof of the first part of Lemma 3.3 since the proof of the second part follows from the same argument.

We start by repeating some of the arguments of the proof of Lemma A.1 with a doubly marked quantum disk $\mathcal{D} = (\mathbf{D}, h, -i, i)$, and we let η be an independent $\text{SLE}_\kappa(3\kappa/2 - 6; -\kappa/2)$ process in \mathbf{D} from $-i$ to i . As a quantum disk is a bead of a quantum wedge of weight $\gamma^2 - 2$, it follows from Theorem B-(ii) that the quantum surfaces parameterized by the components of $\mathbf{D} \setminus \eta$ which are to the left (resp. right) of η are beads of a quantum wedge of weight $3\gamma^2/2 - 4$ (resp. $2 - \gamma^2/2$). In particular, the beads to the left of η are exactly of the type considered in the first part of Lemma 3.3.

Let $x \in \partial\mathbf{D}$ be picked from the quantum length measure independently of everything else. Let η_x be an $\text{SLE}_\kappa(3\kappa/2 - 6; -\kappa/2)$ process in \mathbf{D} from $-i$ to x which is coupled together with η so as to agree

FIGURE 10. The curve η ; the coupling with η_x .

until the first time that their target points have been separated and then to evolve independently afterwards (we also assume that the pair (η, η_x) is independent of \mathcal{D}), see Figure 10. Let \mathcal{B}_x be the bead of $\mathbf{D} \setminus \eta$ with x on its boundary. The target-independence of these $\text{SLE}_\kappa(\rho, \kappa - 6 - \rho)$ processes show readily that the part of η_x in \mathcal{B}_x , viewed as a process starting from the branching point z and which is targeted at the *first* point y on $\partial\mathcal{B}_x$ visited by η , is an $\text{SLE}_\kappa(3\kappa/2 - 6)$ process (here and in the following paragraph, we will implicitly use the fact that x is chosen randomly, and has a positive probability to actually be very close to y). We can actually couple it with an $\text{SLE}_\kappa(3\kappa/2 - 6)$ that goes all the way to y and that we denote by $\tilde{\eta}$.

On the event that x is on the counterclockwise segment of $\partial\mathbf{D}$ from $-i$ to i , the same arguments as above show that the beads parameterized by the components of $\mathbf{D} \setminus \eta_x$ which are to the left (resp. right) of η_x are beads of a quantum wedge of weight $3\gamma^2/2 - 4$ (resp. $2 - \gamma^2/2$). Putting all these items together, one gets that the following is true; Suppose that $\tilde{\mathcal{B}}$ is a bead of a wedge of weight $2 - \gamma^2/2$ (i.e., the same type as \mathcal{B}_x) and $\tilde{\eta}$ is an independent $\text{SLE}_\kappa(3\kappa/2 - 6)$ process between the two marked points of $\tilde{\mathcal{B}}$ (i.e., same law as $\tilde{\eta}$ in \mathcal{B}_x). Then the components which are to the left of $\tilde{\eta}$ are independent given their boundary lengths and are beads of a wedge of weight $3\gamma^2/2 - 4$. To complete the proof, we need to show that the surface which is to the right of $\tilde{\eta}$ is a quantum disk.

If we stop $\tilde{\eta}$ at a time before it reaches its target point and just disconnects a boundary arc to its left (so that it could actually choose to branch to its left at that point) as in Figure 11, then the same argument shows that the surface which is to its right is a bead of a quantum wedge of weight $2 - \gamma^2/2$ (conditionally on its boundary lengths). But as $\tilde{\eta}$ approaches its target point, the left boundary length of this bead tends to 0 while its right boundary length increases. One can then just apply Lemma A.1 to conclude. \square

REFERENCES

- [1] J. Aru, Y. Huang, and X. Sun. Two perspectives of the 2D unit area quantum sphere and their equivalence. *Comm. Math. Phys.*, 356(1):261–283, 2017.
- [2] S. Benoist and C. Hongler. The scaling limit of critical Ising interfaces is CLE_3 . *Ann. Probab.*, 47(4):2049–2086, 2019.
- [3] J. Bertoin. *Lévy processes*, volume 121 of *Cambridge Tracts in Mathematics*. Cambridge University Press, Cambridge, 1996.

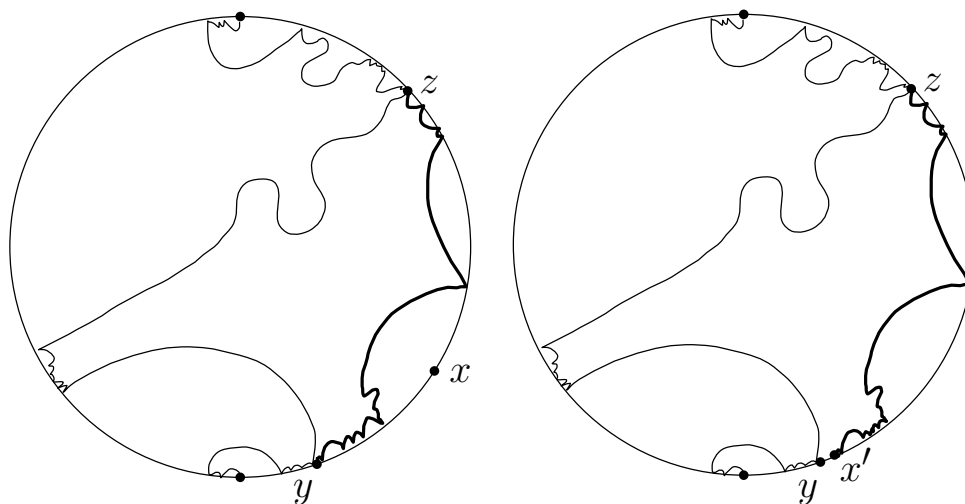


FIGURE 11. The curve $\hat{\eta}$ from z to y in the bead \mathcal{B}_x . The curve just before completion can be viewed as part of $\eta_{x'}$ for x' near y and therefore defines a bead of a wedge on its right.

- [4] J. Bertoin. Markovian growth-fragmentation processes. *Bernoulli*, 23(2):1082–1101, 2017.
- [5] J. Bertoin, T. Budd, N. Curien, and I. Kortchemski. Martingales in self-similar growth-fragmentations and their connections with random planar maps. *Probab. Theory Related Fields*, 172(3-4):663–724, 2018.
- [6] J. Bertoin, N. Curien, and I. Kortchemski. Random planar maps and growth-fragmentations. *Ann. Probab.*, 46(1):207–260, 2018.
- [7] J. Bertoin, N. Curien, and I. Kortchemski. On conditioning a self-similar growth-fragmentation by its intrinsic area. *ArXiv*, 2019.
- [8] J. D. Biggins. Uniform convergence of martingales in the branching random walk. *Ann. Probab.*, 20(1):137–151, 1992.
- [9] J. D. Biggins and A. E. Kyprianou. Measure change in multitype branching. *Adv. in Appl. Probab.*, 36(2):544–581, 2004.
- [10] G. Borot, J. Bouttier, and E. Guitter. A recursive approach to the $O(n)$ model on random maps via nested loops. *J. Phys. A*, 45(4):045002, 38, 2012.
- [11] T. Budd. The peeling process on random planar maps coupled to an $o(n)$ loop model (with an appendix by linxiao chen), 2018.
- [12] B. Cerclé. Unit boundary length quantum disk: a study of two different perspectives and their equivalence. *arXiv e-prints*, page arXiv:1912.08012, Dec 2019.
- [13] L. Chen, N. Curien, and P. Maillard. The perimeter cascade in critical Boltzmann quadrangulations decorated by an $O(n)$ loop model. *Ann. IHP (D)*, to appear.
- [14] N. Curien and L. Richier. Duality of random planar maps via percolation, 2018.
- [15] B. Dadoun. Asymptotics of self-similar growth-fragmentation processes. *Electron. J. Probab.*, 22:Paper No. 27, 30, 2017.
- [16] F. David, A. Kupiainen, R. Rhodes, and V. Vargas. Liouville quantum gravity on the Riemann sphere. *Comm. Math. Phys.*, 342(3):869–907, 2016.
- [17] J. Ding, J. Dubédat, A. Dunlap, and H. Falconet. Tightness of Liouville first passage percolation for $\gamma \in (0, 2)$. *arXiv e-prints*, page arXiv:1904.08021, Apr 2019.
- [18] B. Duplantier, J. Miller, and S. Sheffield. Liouville quantum gravity as a mating of trees. *ArXiv e-prints*, Sept. 2014.
- [19] B. Duplantier and S. Sheffield. Liouville quantum gravity and KPZ. *Invent. Math.*, 185(2):333–393, 2011.
- [20] C. Garban and H. Wu. On the convergence of fk-ising percolation to $\text{sle}(16/3, (16/3)-6)$. *Journal of Theoretical Probability*, Oct 2019.
- [21] E. Gwynne and J. Miller. Chordal SLE_6 explorations of a quantum disk. *Electron. J. Probab.*, 23:Paper No. 66, 24, 2018.

- [22] E. Gwynne and J. Miller. Confluence of geodesics in Liouville quantum gravity for $\gamma \in (0, 2)$. *arXiv e-prints*, page arXiv:1905.00381, May 2019. To appear in *Annals of Probability*.
- [23] E. Gwynne and J. Miller. Conformal covariance of the Liouville quantum gravity metric for $\gamma \in (0, 2)$. *arXiv e-prints*, page arXiv:1905.00384, May 2019.
- [24] E. Gwynne and J. Miller. Existence and uniqueness of the Liouville quantum gravity metric for $\gamma \in (0, 2)$. *arXiv e-prints*, page arXiv:1905.00383, May 2019.
- [25] E. Gwynne and J. Miller. Local metrics of the Gaussian free field. *arXiv e-prints*, page arXiv:1905.00379, May 2019. To appear in *Annales de l'Institut Fourier*.
- [26] R. Høegh-Krohn. A general class of quantum fields without cut-offs in two space-time dimensions. *Comm. Math. Phys.*, 21:244–255, 1971.
- [27] Y. Huang, R. Rhodes, and V. Vargas. Liouville quantum gravity on the unit disk. *Ann. Inst. Henri Poincaré Probab. Stat.*, 54(3):1694–1730, 2018.
- [28] J.-P. Kahane. Sur le chaos multiplicatif. *Ann. Sci. Math. Québec*, 9(2):105–150, 1985.
- [29] A. Kemppainen and S. Smirnov. Conformal invariance in random cluster models. II. Full scaling limit as a branching SLE. *arXiv e-prints*, page arXiv:1609.08527, Sep 2016.
- [30] J.-F. Le Gall and G. Miermont. Scaling limits of random planar maps with large faces. *Ann. Probab.*, 39(1):1–69, 2011.
- [31] Q. Liu. On generalized multiplicative cascades. *Stochastic Process. Appl.*, 86(2):263–286, 2000.
- [32] R. Lyons, R. Pemantle, and Y. Peres. Conceptual proofs of $L \log L$ criteria for mean behavior of branching processes. *Ann. Probab.*, 23(3):1125–1138, 1995.
- [33] J. Miller and S. Sheffield. Imaginary geometry I: interacting SLEs. *Probab. Theory Related Fields*, 164(3-4):553–705, 2016.
- [34] J. Miller and S. Sheffield. Imaginary geometry II: reversibility of $\text{SLE}_\kappa(\rho_1; \rho_2)$ for $\kappa \in (0, 4)$. *Ann. Probab.*, 44(3):1647–1722, 2016.
- [35] J. Miller and S. Sheffield. Liouville quantum gravity and the Brownian map II: geodesics and continuity of the embedding. *arXiv e-prints*, page arXiv:1605.03563, May 2016.
- [36] J. Miller and S. Sheffield. Liouville quantum gravity and the Brownian map III: the conformal structure is determined. *arXiv e-prints*, page arXiv:1608.05391, Aug 2016.
- [37] J. Miller and S. Sheffield. Liouville quantum gravity and the Brownian map I: The QLE(8/3,0) metric. *Inventiones Math.*, to appear.
- [38] J. Miller, S. Sheffield, and W. Werner. Non-simple conformal loop ensembles on Liouville Quantum Gravity. *in preparation*.
- [39] J. Miller, S. Sheffield, and W. Werner. CLE percolations. *Forum Math. Pi*, 5:e4, 102, 2017.
- [40] J. Miller, S. Sheffield, and W. Werner. Non-simple SLE curves are not determined by their range. *J. Europ. Math. Soc.*, 22:669716, 2020.
- [41] S. Nacu and W. Werner. Random soups, carpets and fractal dimensions. *J. Lond. Math. Soc. (2)*, 83(3):789–809, 2011.
- [42] R. Robert and V. Vargas. Gaussian multiplicative chaos revisited. *Ann. Probab.*, 38(2):605–631, 2010.
- [43] S. Rohde and O. Schramm. Basic properties of SLE. *Ann. of Math. (2)*, 161(2):883–924, 2005.
- [44] O. Schramm. Scaling limits of loop-erased random walks and uniform spanning trees. *Israel J. Math.*, 118:221–288, 2000.
- [45] O. Schramm, S. Sheffield, and D. B. Wilson. Conformal radii for conformal loop ensembles. *Comm. Math. Phys.*, 288(1):43–53, 2009.
- [46] S. Sheffield. Exploration trees and conformal loop ensembles. *Duke Math. J.*, 147(1):79–129, 2009.
- [47] S. Sheffield. Conformal weldings of random surfaces: SLE and the quantum gravity zipper. *Ann. Probab.*, 44(5):3474–3545, 2016.
- [48] S. Sheffield and M. Wang. Field-measure correspondence in Liouville quantum gravity almost surely commutes with all conformal maps simultaneously. *arXiv e-prints*, page arXiv:1605.06171, May 2016.
- [49] S. Sheffield and W. Werner. Conformal loop ensembles: the Markovian characterization and the loop-soup construction. *Ann. of Math. (2)*, 176(3):1827–1917, 2012.
- [50] S. Smirnov. Conformal invariance in random cluster models. I. Holomorphic fermions in the Ising model. *Ann. of Math. (2)*, 172(2):1435–1467, 2010.
- [51] W. Werner and H. Wu. On Conformally Invariant CLE Explorations. *Communications in Mathematical Physics*, 320:637–661, 2013.

STATSLAB, CENTER FOR MATHEMATICAL SCIENCES, UNIVERSITY OF CAMBRIDGE, WILBERFORCE ROAD, CAMBRIDGE
CB3 0WB, UK

E-mail address: `jpmiller@statslab.cam.ac.uk`

DEPARTMENT OF MATHEMATICS, MIT, 77 MASSACHUSETTS AVENUE, CAMBRIDGE, MA 02139, USA

E-mail address: `sheffield@math.mit.edu`

DEPARTMENT OF MATHEMATICS, ETH ZÜRICH, RÄMISTR. 101, 8092 ZÜRICH, SWITZERLAND

E-mail address: `wendelin.werner@math.ethz.ch`